

博士論文

**KLF15 suppresses mammalian cancer cell growth via interaction
with PKM2**

(**KLF15** は **PKM2** との相互作用を介して乳がん細胞の増殖
を抑制する)

ま えんか

馬 艶霞

Ma Yanxia

Contents

Abbreviation	4
Abstract	7
Introduction	9
Purpose	17
Materials and Methods	18
Ethical Approval	18
Reagents and Antibodies	18
Cell Culture and Establishment of Stable Tumor Cell Lines.....	19
Plasmid Construction.....	20
Preparation of Protein Extracts.....	21
Immunoprecipitation (IP) and Western Blotting Assay.....	22
Mass Spectrometry Analysis	23
Reporter Gene Assay	23
Recombinant Adenovirus Infection.....	24
Reverse Transcription PCR (RT-PCR) and Quantitative RT-PCR (qRT-PCR)	
Analysis	25
Immunocytochemical Analysis.....	25
Cell Proliferation Analysis.....	26
In Vitro Wound Healing Analysis.....	27
FACS Analysis of the Cell Cycle Distribution	27
Xenograft Transplantation of Tumor Cells	28
Immunohistochemical Analysis of Human Breast Tissues.....	29
Statistical Analysis.....	29
Results	31
1. PKM2 is a novel interacting partner of KLF15	31
2. KLF15 shows cell type-dependent expression profile	31
3. KLF15-PKM2 interaction downregulates β-catenin-dependent reporter gene	
expression in breast cancer cell.....	32
4. PKM2/β-catenin-downstream factors and cell cycle regulators are inhibited by	
KLF15 overexpression in stably transfected MCF7 cells	33
5. Overexpression of KLF15 downregulates cell distribution in G2/M phase, inhibits	
cell proliferation and migration	35

6. KLF15 suppresses breast cancer cell xenograft growth	36
7. Expressions of KLF15 and PKM2 show an inverse association in human breast carcinoma	37
Discussion	38
Conclusion	43
References	44
Tables and Figures	55
Table 1. Features of Molecular Subtypes of Breast Cancer	55
Table 2. Reasonable recommendations – personalizing the treatment of women with early breast cancer: 13 th St Gallen 2013	56
Table 3. Reasonable recommendations – personalizing the treatment of women with early breast cancer: 13 th St Gallen 2013	57
Table 4. List of Plasmids	58
Table 5. Oligonucleotide DNA Template and Insert Enzyme Sites for short hairpin RNA (shRNA) Plasmid	59
Table 6. Primers and Insert Enzyme Sites for Expression Plasmid (1)	60
Table 6. Primers and Insert Enzyme Sites for Expression Plasmid (2)	61
Table 7. Primers for DNA Sequencing	62
Table 8. Primers for qRT-PCR (human)	63
Table 9. Candidates of KLF15 Interaction Factor	64
Table 10. Association between immunohistochemical KLF15 and PKM2 status in human breast carcinoma	65
Figure 1. PKM2 is a candidate of KLF15-interacting partners.....	66
Figure 2. KLF15 interacts with PKM2 in human breast cancer cells.	67
Figure 3. mRNA and protein expression profiles of KLF15 and PKM2 in various human cell lines	69
Figure 4. Subcellular localization of KLF15 and PKM2 in human breast cancer cells	70
Figure 5. KLF15 interacts with N-terminal region (amino acids 1-377) of PKM2	72
Figure 6. KLF15-PKM2 interaction downregulates β -catenin-dependent reporter gene expression in breast cancer cells	74
Figure 7. KLF15 and PKM2 regulate expression levels of several cellular proteins in human breast cancer cells.....	76

Figure 8. KLF15 and PKM2 regulate cell cycle distribution of human breast cancer cells.....	78
Figure 9. Either KLF15 overexpression or PKM2 knockdown suppresses breast cancer cell proliferation and migration.....	80
Figure 10. Xenograft transplantation of stably transfected MCF7 cells into NOD-SCID mice	82
Figure 11. KLF15 suppresses and PKM2 promotes xenografted breast tumor growth in NOD-SCID mice	84
Figure 12. Immunohistochemical analysis of KLF15 and PKM2 in human breast carcinoma and normal mammary gland tissues.....	86
Acknowledgements	87

Abbreviation

KLF15	Krüppel-like factor-15
KLF	Krüppel-like family of transcription factors
NLS	Nuclear localization signal
MCM2	Mini-chromosome maintenance protein 2
MYC	MYC gene encoding for c-Myc
CDK2	Cyclin-dependent kinases 2
E2F1	E2F transcription factor 1
mRNA	Messenger ribonucleic acid
G418	Geneticin
DAB	3,30-diaminobenzidine tetrahydrochloride
JMJD5	Jumonji C domain-containing dioxygenase
ATP	Adenosine triphosphate
ADP	Adenosine diphosphate
PTBP1	Polypyrimidine-tract binding protein1
FBP	Fructose-1, 6-bisphosphate
TCA	Tricarboxylic acid

NF- κ B	Nuclear factor kappa enhancer binding protein
HIF-1 α	Hypoxia-inducible factor 1 α
PI3K	Phosphoinositide 3-kinase
mTOR	Mammalian (or mechanistic) target of rapamycin
MMPs	Matrix metalloproteinases
EGFR	Epidermal growth factor receptor
MSCs	Mammary stem cells
PML	Promyelocytic leukemia
PML-NBs	PML nuclear bodies
cPML	Cytoplasmic PML
TRAF4	Tumor necrosis factor receptor-associated factor 4
IGFIR	Insulin-like growth factor receptor
TNBC	Triple-negative breast cancer
IGF1R	Insulin-like growth factor receptor
PKM2	M2 type pyruvate kinase
PKM1	M1 type pyruvate kinase
ROS	Reactive oxygen species

shRNA	Short hairpin RNA
MMP2	Matrix metalloproteinase 2
ROR2	Receptor tyrosine kinase-like orphan receptor 2
UPP	Ubiquitin-proteasome pathway
TCF/LEF	DNA-bound T cell/lymphoid enhancer factor
NOD-SCID	Non-Obese Diabetic-Severe Combined Immunodeficiency

Abstract

Breast cancer is one of the most common malignant diseases and the second leading cause of cancer related mortalities in women worldwide. Krüppel-like factor (KLF15), a nuclear transcription factor, has been reported as an inhibitor of cell proliferation via modulating the expression of cell cycle regulatory factors, including E2F1, cyclin D1, CDK2 and MCM2. However, the functions of KLF15 in cancer biology and the associated molecular regulatory networks remain to be understood.

In present study, M2 pyruvate kinase (PKM2) was identified as a novel interacting partner of KLF15. High expression level of PKM2 indicates poor prognosis and high rate of recurrence in breast cancers. Nuclear PKM2 has been reported to show non-metabolic functions, acting as a coactivator within the Wnt/ β -catenin/c-Myc/PTBP1 signaling pathway. Our study demonstrated that KLF15 contributed to downregulation of PKM2-driven Wnt/ β -catenin/c-Myc/PTBP1 signaling network in breast cancer-derived cell lines. Overexpression of KLF15 resulted in enhanced cell population in G0/G1/S phase along with decreased cell proportion in G2/M phase. Moreover, KLF15 suppressed breast cancer cell proliferation and migration, showing the converse actions to PKM2. In NOD-SCID mice, overexpression of KLF15 suppressed MCF7 cell xenograft growth. Immunohistochemical

analysis of KLF15 and PKM2 in pathological specimens obtained from patients with breast carcinoma indicated an inverse association between the expression of KLF15 and PKM2.

Taken together, we may conclude that KLF15 is a potential suppressor of breast cancer cell growth. Anti-proliferative effect of KLF15 might at least in part be through interactions with nuclear PKM2 and thereby inhibiting nuclear PKM2 signaling network.

Introduction

Breast cancer is the most common malignant disease in women and the second leading cause of cancer related mortalities in women worldwide. In 2011, over 508,000 women died of breast cancer worldwide ⁽¹⁾. Based on current incidence rate, a woman has 1 in 8 chance of being diagnosed with breast cancer during the lifetime ⁽²⁾.

Breast cancer is divided into categories according to different schemes and based on different criteria (**Table 1 and 2**) ⁽³⁾. The major categories include the grade of the tumor, the stage of the tumor, histopathological type, and the expression of proteins and genes. The purpose of classification is to select the best treatment. For example, the “13th St Gallen International Expert Consensus on the Primary Therapy of Early Breast Cancer 2013” proposed new classification for personalizing the treatment of women with early breast cancer. According to that report, breast cancer is divided into 4 subtypes based on the clinico-pathological surrogate makers, and luminal B-like is further divided into 2 groups depended on HER2 expression for adaptation of systemic treatment (**Table 2 and 3**).

Approximately 70% of invasive breast cancers are classified as ER and/or PR positive (luminal A or B), which could be a predictor that the relevant patient will likely benefit from hormone therapy ⁽⁴⁾. The strategies for hormone therapy in hormone receptor-positive breast

cancer include blocking estrogen production by ovarian ablation, treatment with aromatase inhibitors (for example, anastrozole) for postmenopausal women, and blocking estrogen's effect by selective estrogen receptor modulators (SERMs) (such as: tamoxifen)⁽⁵⁾. However, a subset of ER-positive breast cancers do not benefit from hormonal therapy because of intrinsic resistance. Moreover, a large number of patients receiving hormonal therapy will eventually develop resistance to the therapy, which is termed acquired resistance⁽⁶⁾. Patients with HER2-positive cancer will more likely benefit from anthracycline and taxane-based chemotherapies, as well as HER2-targeted therapies, such as trastuzumab, but not from hormonal therapies⁽⁶⁻⁷⁾. Triple-negative breast cancer (TNBC) is believed to originate from mammary stem cells (MSCs) and is associated with poor clinical outcome. At present, it's difficult to develop effective targeted therapies for metastatic TNBC⁽⁸⁾. Further characterization of molecular mechanism of tumorigenesis and cancer progression would provide valuable targets for developing novel therapeutic strategies, and benefit breast cancer patients.

It is becoming clear that not only hormone receptors but also other cellular components can critically modulate the biological characteristics of breast cancer cells. For example, β -catenin and M2 pyruvate kinase (PKM2) signaling pathways have been increasingly

highlighted in breast tumor biology.

β -catenin is a transcriptional coactivator, which can be activated by canonical Wnt signaling pathway. In the absence of Wnt signaling, β -catenin protein is constantly eliminated by ubiquitin-proteasome pathway (UPP) in the cytoplasm. When Wnt signaling is activated, β -catenin protein is protected from degradation, and translocates into the nucleus to form complexes with DNA-bound T cell/lymphoid enhancer factor (TCF/LEF) and activates key gene expression programs ⁽⁹⁾.

It has been reported that β -catenin signaling mediates the tumorigenesis and maintenance of breast cancers. Enhanced activity of β -catenin signaling is linked to recurrent or metastatic breast cancer through mediating the function of commonly overexpressed breast cancer oncogenes, such as Recepteur d'Origine Nantaise (Ron) and DEK oncogene (a novel nuclear effector of Ron activation) ⁽¹⁰⁾. Tumor necrosis factor receptor-associated factor 4 (TRAF4) interacts with β -catenin, and mediates nuclear localization of β -catenin, which facilitates activation of the Wnt signaling pathway in breast cancer ⁽¹¹⁾. Since inhibitors of insulin-like growth factor receptor (IGF1R) downregulate Wnt/ β -catenin activation, they are suggested to treat TNBC ⁽¹²⁾. In breast cancer, activation of β -catenin signaling stimulated by interleukin 1 β led to elevated expression of c-Myc, G1/S-specific cyclin D1, transcription factor

Snail1 and matrix metalloproteinase 2 (MMP2) ⁽¹³⁾. Activation of β -catenin signaling also upregulated miR-29 expression, contributing to decreased level of N-myc interactor (NMI), therefore, increased invasion of breast cancer cells ⁽¹⁴⁾. Breast cancer patients expressing receptor tyrosine kinase-like orphan receptor 2 (ROR2) show a significantly worse prognosis. β -catenin-dependent Wnt pathway has been reported to mediate the effect of ROR2, which implies yet again the important role of β -catenin signaling in breast cancer ⁽¹⁵⁾.

It has been highlighted that PKM2 associates with cancer biology. In cancer cells, glucose uptake and lactate production are significantly increased, accompanied by inhibited phosphorylation process regardless of oxygen availability. This metabolic phenomenon is termed aerobic glycolysis or Warburg effect, which allows tumor cells to synthesize macromolecules (amino acids, phospholipids, and nucleic acids) using a large fraction of glucose metabolites ⁽¹⁶⁾. It has been believed that PKM2 localizes in the cytoplasm and acts as a glycolytic enzyme to mediate Warburg effect in tumor ⁽¹⁶⁻¹⁹⁾. In cytoplasm, dimer-tetramer transition of PKM2 is allosterically regulated by Fructose-1, 6-bisphosphate (FBP), which is a glycolysis metabolic intermediate. Both dimeric and tetrameric PKM2 catalyze the final rate-limiting step of glycolysis to produce pyruvate molecule through dephosphorylation of phosphoenolpyruvate. Moreover, PKM2 is responsible for the production of adenosine

triphosphate (ATP) within the glycolysis process. Pyruvate catalyzed by the tetrameric PKM2 enters into TCA cycle, favoring ATP production. The less active dimeric PKM2, however, leads to high levels of lactate production and lower oxygen consumption, which is crucial for Warburg effect in tumor cells ⁽¹⁸⁾. Recent studies also indicated that PKM2 enters into the nucleus and takes part in transcriptional regulation of gene expression. Nuclear PKM2 interacts with p300 and hypoxia-inducible factor1 (HIF-1 α) to the form PKM2/HIF-1 α feedforward loop in tumor ⁽²⁰⁻²¹⁾. Moreover, nuclear PKM2 interacts with β -catenin and upregulate expression of c-Myc and polypyrimidine tract-binding protein 1 (PTBP1) to form PKM2/ β -catenin/c-Myc positive feedback loop in tumor ⁽²²⁾. Thus, both cytoplasmic and nuclear PKM2 are involved in formation and progression of cancer.

In breast cancer, it has been reported that PKM2 directly interacts with Jumonji C domain-containing dioxygenase (JMJD5) ⁽²³⁾ in the nucleus and with promyelocytic leukemia (PML) tumor suppressor protein ⁽²⁴⁾ in the cytoplasm, to mediate the functions of JMJD5 and PML tumor suppressor protein. In breast cancer cell lines, MDA-MB-231 and MCF7, PKM2 is involved in regulation of apoptosis and ATP levels ⁽²⁵⁾. Moreover, effects of PTBP1 on tumor cell growth and the maintenance of transformed properties are mediated, at least in part, by regulating mRNA splicing of PKM gene and promoting expression of PKM2 ⁽²⁶⁾.

Furthermore, in stromal fibroblasts, expression of PKM2 mediates the “Reverse Warburg Effect” in breast cancer and promotes growth of MDA-MB-231 breast cancer cells in a xenograft model ⁽²⁷⁻²⁸⁾. It has been reported that Shikonin, an inhibitor of PKM2 activity, combining with taxol, shows anti-cancer effect in human breast adenocarcinoma MDA-MB-231 cells ⁽²⁹⁾.

Our study focused on Krüppel-like factor 15 (KLF15), a nuclear transcription factor. KLF15 was first reported as a repressor of the kidney-specific chloride channel gene CLC-K1 ⁽³⁰⁾. The mRNA sequence homology of KLF15 among human, mouse and rat are 83.4% in human vs mouse, 83.8% in human vs rat, and 95.9% in mouse vs rat. KLF15 belongs to the Krüppel-like family of nuclear transcription factors. All KLF proteins contain a DNA-binding domain (DBD) consisting of three Cys2-His2 zinc finger motifs at their carboxyl-terminal end. KLF15 binds to GC-rich sequences (“CACCC” sequence, or “GGGGNGGNG” sequence) of target gene through those three zinc fingers ⁽³¹⁻³²⁾. Since KLF15 lacks the classical nuclear localization signal (NLS), but C-terminal region of KLF15 which containing three zinc fingers acts as the NLS ⁽³²⁾. It has been reported that KLF15 is a metabolic regulatory factor in liver, muscle and adipose tissues, acting as a central component for coordinating physiologic flux of glucose, amino acids, and lipids ⁽³³⁾. Moreover, functions of KLF15 in cardiovascular

system have been revealed as well. Via binding with myocardin or myocardin-related transcription factors (MRTF-A, MRTF-B), KLF15 inhibits the activity of myocardin or MRTFs in heart and aorta, and provides therapeutic implications for cardiac diseases⁽³⁴⁻³⁵⁾; via interacting with p300, KLF15 represses p300-dependent acetylation of NF- κ B, leading to suppressive activation of NF- κ B in vascular smooth muscle⁽³⁶⁾.

Furthermore, prior investigations shed light on the anti-proliferative effect of KLF15 in cells. KLF15 inhibits cultured mesangial cell proliferation by regulating the expression of cell cycle regulatory proteins, including E2F transcription factor 1 (E2F1), cyclin D1 and cyclin-dependent kinase 2 (CDK2)⁽³⁷⁾. Overexpression of KLF15 reduces proliferation of human airway smooth muscle cells⁽³⁸⁾. Additionally, KLF15 inhibits growth and transformation induced by oncogenic V-Ki-ras2 Kirsten rat sarcoma viral oncogene homologue (KRAS) in human pancreas adenocarcinoma (BxPC-3) cells⁽³⁹⁾. Of note, KLF15 shows an inhibitory effect on estrogen-induced proliferation of epithelial cells, Ishikawa cell (an ER and PR positive human endometrial adenocarcinoma cell line), as well as ER-positive T47D breast cancer cells, by downregulating Mini-chromosome maintenance protein 2 (MCM2) protein level⁽⁴⁰⁾. Given these pleiotropic functions of KLF15 in cell growth and proliferation, especially the anti-proliferative effect on T47D cells, we decided to study the

role of KLF15 in breast cancer.

We here show that PKM2 is a novel interacting factor of KLF15. KLF15 and PKM2 show converse effects on breast cancer cell growth and migration, as well as cell cycle reprogramming. KLF15 may inhibit nuclear PKM2 signaling network, and therefore acts as a potential suppressor of breast cancer cell growth.

Purpose

Pioneering investigations have revealed that KLF15 mediates anti-proliferative effect on diverse cancer cell lines. However, the effect of KLF15 in breast cancer biology remains unclear. In light of previous observation, we performed a series of analysis to explore the roles of KLF15 in breast cancer, including:

1. To identify the interacting partners of KLF15,
2. To define the domains of KLF15 and partner(s) that are critical for the interaction,
3. To explore the functions of KLF15 in cofactor-associated signaling pathways,
4. To establish stable breast cancer cell lines that express KLF15 or cofactors at various levels,
and to explore functional characterization of stably transfected breast cancer cell lines,
5. To investigate the effect of KLF15 and cofactor on breast cancer cell xenograft growth in
Non-Obese Diabetic-Severe Combined Immunodeficiency (NOD-SCID) mice,
6. To investigate the expression of KLF15 and cofactor in non-neoplastic human breast
tissues and human breast carcinoma tissues.

Materials and Methods

Ethical Approval

The transplantation experiments using MCF-7 cell lines and NOD/SCID mice were approved by Animal Experiment Ethics Committee of National Center of Neurology and Psychiatry, Kodaira, Tokyo, Japan (Approval Number: 2013008).

Research protocols for the study related to pathological specimens from human breast carcinoma patients were approved by the Ethics Committee of the Tohoku University School of Medicine, Sendai, Japan (Approval Number: 2013-1-437).

Reagents and Antibodies

Reagents were obtained from Nacalai Tesque (Kyoto, Japan) unless otherwise specified.

MG-132 (M7449), Anti-FLAG[®] M2 antibody (F3165) and affinity agarose gel (A2220), anti- α -Tubulin antibodies (T5168), and FLAG[®] peptide (F3290) were obtained from Sigma-Aldrich (St. Louis, MO). Anti-PKM2 (D78A4), CDK2 (78B2), MCM2 (4007s), PTBP1 (8776s), and PCNA (2586) antibodies, and horseradish peroxidase (HRP)-conjugated mouse anti-rabbit IgG monoclonal antibody (5127) were obtained from Cell Signaling Technology (Beverly, MA). Anti-c-Myc antibodies (SC-764) and donkey anti-goat IgG-HRP

(sc-2020) were obtained from Santa Cruz Biotechnology (Santa Cruz, CA). Anti-KLF15 antibodies (NBP1-82872) were obtained from Novus Biologicals (Littleton, CO). Anti- β -actin (ab1801) and HA (ab18181) antibodies were obtained from Abcam (Cambridge, UK). HRP-conjugated anti-mouse (NA931V) and rabbit (NA934V) secondary antibodies, and Protein G/A sepharose™ 4 fast flow (17-5280-01) were obtained from GE Healthcare (Little Chalfont, UK).

Cell Culture and Establishment of Stable Tumor Cell Lines

C2C12 mouse myoblasts, A549 human lung carcinoma, HEK293 human embryonic kidney, HeLa human cervix adenocarcinoma, HepG2 human hepatocellular carcinoma, and human breast cancer cells (MCF7, T47D, MDA-MB-231, ZR-75-1, and BT-20) were obtained from American Type Culture Collection (ATCC, Manassas, VA). Human breast cancer cells and the other cells were maintained in RPMI-1640 (with L-Glutamine and Phenol Red, 188-02025, Wako, Saitama, Japan) or DMEM (High Glucose, 08459-35, Nacalai Tesque), respectively, supplemented with 10% fetal bovine serum (Biowest, Nuaille, France) along with 1% penicillin and streptomycin mixed solution (26253-84, Nacalai Tesque) in a humidified atmosphere at 37°C with 5% CO₂. The culture medium was replaced with fresh one every 2 days and the cells were passaged before they reach confluence.

For establishment of stably transfected cell lines, transfection of the expression plasmids carrying neomycin-resistant gene was performed with TransIT[®]-LT1 Low Toxicity Reagent (MIR 2300, Mirus Bio Corp., Madison) according to the manufacturer's instructions. Cells were treated with 400 μ g/ml of G418 (10131027, Geneticin, Life Technologies) for 3-4 weeks. After antibiotic-resistant colonies became apparent, single cell screening was performed by culture in 96-well plates. Individual colonies were picked, pooled and expanded for further analysis under selective conditions with 150 μ g/ml G418.

Plasmid Construction

A series of plasmids were constructed as shown in **Table 4**. To construct the expression plasmids for short hairpin RNA (shRNA) against human KLF15 (pSilencer-shRNA-hKLF15) and human PKM2 (pSilencer-shRNA-hPKM2), shRNA template oligonucleotides (listed in **Table 5**) were annealed and inserted into pSilencer3.1[™]-H1 neo vector (Life technologies) at BamHI/HindIII enzyme sites. To construct the expression plasmids for mouse PKM1 and PKM2, as well as human PKM2 and KLF15, mouse and human cDNAs were generated from mRNA obtained from mouse brain and C2C12, HeLa, and HepG2 cells by using oligo-dT primers and reverse transcriptases. Using them as a template, cDNAs of mouse PKM1, PKM2 and KLF15, as well as human PKM2 and KLF15 were generated by PCR amplification with

target gene specific primers listed in **Table 5** and subcloned into pCMX-Flag, pCMX-HA⁽⁴¹⁾, or p3×Flag-CMV10 (Sigma-Aldrich) respectively. To construct various N-terminal and C-terminal-truncated mutants of KLF15 and PKM2, appropriate PCR fragments were generated with specific primers listed in **Table 6** and inserted into pCMX-Flag, pCMX-HA, or p3×Flag-CMV-10. Expression plasmid for β -catenin and β -catenin-dependent reporter plasmids, TOP-Flash (wild-type) and FOP-Flash (mutant of responsive element), were kindly gifted from Dr. Yuki Ikeda (Division of Molecular Pathology, Institute of Medical Science, The University of Tokyo, Tokyo, Japan)⁽⁴²⁾. Sequences of these constructs were confirmed by DNA sequencing (primers used for DNA sequencing listed in **Table 7**).

Preparation of Protein Extracts

Whole cell extracts were prepared in NP-40 lysis buffer (3 ml of 5 M NaCl, 10ml of 10% NP-40, 5ml of 1M Tris pH8.0, in 100ml distilled water) supplemented with 1 mM dithiothreitol, 100 nM MG132, protease inhibitor cocktail and phosphatase inhibitor cocktail. They were incubated on ice for 15 min followed by centrifugation for 20 min at 20,000 x g and soluble fractions were used as whole cell extracts. Cytosol and nuclear extracts were prepared as previously described with minor modification⁽⁴³⁾. The cell pellets were incubated with lysis buffer A (10mM HEPES pH8.0, 10mM KCl, 0.1mM EDTA pH 8.0, 0.1mM

EGTA) with 0.6% NP-40 on ice for 5 min. Then, cell lysates were centrifuged and the supernatant was used as cytosol, the residual pellets were resuspended in lysis buffer C (20mM HEPE pH 8.0; 400mM NaCl; 1mM EDTA pH 8.0; 1mM EGTA) on ice for 30 min, and followed by centrifugation at 12,000 x g for 15 min (4°C). The supernatant was used as nuclear extracts. Protein concentration of each sample was measured using BCA protein assay kit (23227, Pierce, Rockford, IL).

Immunoprecipitation (IP) and Western Blotting Assay

For immunoprecipitation assay, cell extracts were incubated with anti-FLAG agarose beads or indicated antibodies for 18-24 hr at 4°C. The cell extracts incubated with indicated antibodies were further incubated with Protein G-Sepharose for 1.5-2.5 hr at 4°C. After washing the beads and antibody mixture with TBS buffer (50mM Tris-HCl, pH 7.4, with 300 mM NaCl) at least three times, bound proteins were eluted with Flag peptides or SDS-sample loading buffer, followed by western blotting analysis.

For western blotting analysis, protein samples were separated by electrophoresis in 7.5%-18% Tris/glycine/SDS-polyacrylamide gel (Glycine: 077-00735, Wako) or 18%-20% Tris/Tricine/SDS-polyacrylamide gel (Tricine: 02437-24, Nacalai Tesque). Electrophoretically resolved proteins were transferred onto polyvinylidene difluoride

membranes (IPVH00010, Millipore, Billerica, MA). Subsequently, immunoblotting was performed with indicated antibodies diluted at 1:500-1:2,000, followed by HRP-conjugated secondary antibodies (diluted at 1:2,000). Antibody-protein complexes were visualized using the enhanced chemiluminescence method according to the manufacturer's protocol (signal enhancer HIKARI, 02270-81, Nacalai Tesque) and images were captured by Luminoimage Analyzer LAS-1000mini (Fujifilm, Tokyo, Japan).

Mass Spectrometry Analysis

After immunoprecipitation of nuclear extracts from cells, the protein samples were subjected to electrophoresis or mass spectrometry analysis. For silver staining analysis, sample was separated by 7.5%-10% Tris/glycine/ SDS-polyacrylamide gel, followed by silver staining analysis according to the manufacturer's protocol (Pierce[®] silver stain for Mass spectrometry, Thermo Scientific, Schwerte, Germany). For mass spectrometry analysis, sample was submitted to In-solution Tryptic Digestion and Guanidination Kit (89895, Thermo Scientific), followed by mass spectrometry analysis with nanoLC-ESI-Q-TOF mass spectrometer (Bruker Daltonik, Bremen, Germany).

Reporter Gene Assay

In reporter gene assay, cells were transiently transfected with reporter plasmids along

with various protein expression plasmids. The total amount of the plasmids was kept constant by adding an irrelevant plasmid. Thereafter, cells were harvested and whole cell extracts were prepared in Cell Culture Lysis Reagent (E1531, Promega, Madison, WI). Luciferase enzyme activity was determined using the Luciferase Assay System (Promega) and luminometer (Promega) according to the manufacturer's protocol. Relative light units were normalized to the protein amounts determined with BCA Protein Assay Reagent. All experiments were performed at least three times in triplicate.

Recombinant Adenovirus Infection

Recombinant adenoviruses encoding Flag-tagged rat KLF15 and Cre-recombinase were generated by using the Adenovirus Cre/loxP-regulated Expression Vector Set (6151, TaKaRa, Otsu, Japan) according to the manufacturer's instructions and following the procedure as previously described ⁽⁴⁴⁾. Recombinant adenoviruses prepared from HEK293 cells were purified with Virakit AdenoMini-24 (003059, Virapur, San Diego, CA) and titrated using an Adeno-X Rapid Titer Kit (632250, TaKaRa). For adenovirus infection, cell culture medium was replaced with fresh medium containing Cre-recombinase expressing adenoviruses with or without Flag-tagged rat KLF15 expressing adenoviruses at an indicated multiplicity of infection, thereafter, cells were further cultured for 24-72 hr at 37°C. Efficacy of adenovirus

infection was estimated by western blotting or quantitative reverse transcription PCR analysis.

Reverse Transcription PCR (RT-PCR) and Quantitative RT-PCR (qRT-PCR) Analysis

Total RNA was extracted from cells using Sepasol-RNA I Super G (09379-84, Invitrogen). cDNA was synthesized by reverse-transcription with SuperScript III First-Strand Synthesis System for RT-PCR (18080-051, Invitrogen). RT-PCR was performed using a platinum[®] PCR SuperMix High Fidelity kit (12532-016, Invitrogen) in Gene Amp[®] PCR system 9700. For qRT-PCR, synthesized cDNAs were subjected to Real-time PCR with SYBR[®] Green Realtime PCR Master Mix (QPK-201, TOYOBO CO., LTD. Life Science Department, Osaka, Japan) and Roche Real-time LightCycler 2.0 System in CFX96[™] Real-Time PCR Detection System (Bio-Rad). On the basis of standard curves generated for each gene, expression levels of mRNA were normalized with housekeeping β -actin. The primer pairs used in qRT-PCR analysis are listed in **Table 8**. All experiments were performed at least three times in triplicate.

Immunocytochemical Analysis

For immunocytochemistry assay, cells were grown on collagen coated coverslips (354108, BD Falcon[™] Culture Slides, BD Biosciences) or 24-well plate (A11428-02,

collagen I coated plate, Life Technologies), fixed in 4% paraformaldehyde fixative (160-00515, Muto Pure Chemicals CO. LTD, Tokyo, Japan) at 37°C for 20 min, incubated with permeabilization buffer (1×PBS, 0.25% TritonX-100) for 15 min at room temperature (RT), and blocked with blocking solution (1×PBS with 0.1% Tween 20 and 5% BSA) for 1 hr at RT. Thereafter, cells were incubated with primary antibodies (1:100 dilution) at 4°C for 18-24 hr, followed with secondary antibodies (1:1000 dilutions) (RPN1004, biotinylated anti-rabbit IgG, GE Healthcare), and third antibodies (RPN1051, Streptavidin-Biotinylated Horseradish Peroxidase Complex, GE Healthcare) at RT for 30 min respectively. The antigen-antibody complex was visualized with mental enhanced DAB substrate kit (34065, Thermo Scientific). Microscopic images were captured with a light microscope (Nikon TE200, Nikon, Tokyo, Japan) and a digital camera (D5300, Nikon).

Cell Proliferation Analysis

Cells were seeded in 96-well plates with a density of 5×10^3 cells/well/100 μ l and incubated for indicated period at 37°C and 5% CO₂. The wild-type cells or cells stably transfected with blank vectors were served as controls. Cell proliferation analysis was assessed by counting number of living cells using the Cell Counting Kit-8 (CCK-8, Dojindo, Japan) according to the manufacturer's protocol. Absorbance of cell plates was read using an

iMark™ microplate Reader (BIO-RAD) at a wavelength of 450 nm. The proliferation ratio was calculated by normalizing OD value at indicated time points with that at 24 hr-time point.

All experiments were performed at least three times in triplicate.

In Vitro Wound Healing Analysis

Directional cell migration and interaction was studied by using an in vitro wound healing analysis ⁽⁴⁵⁻⁴⁶⁾. Stably transfected MCF7 cells were seeded in 6-well tissue culture plates and grown to 100% confluence. Wounds were created by scraping the monolayer of the cells with a sterile pipette 200 μ l-tip. The images of wounds were captured at 4 \times magnification with a Nikon TE200 microscope with Nikon D5300 camera immediately after wounding, as well as 24 and 48 hours later. The wound area was analyzed by using “Wound Healing Assay Tool” of Image J software.

FACS Analysis of the Cell Cycle Distribution

Stably transfected MCF7 cells were plated at a density of 1.0-1.5 $\times 10^6$ /dish in 60 mm-diameter tissue culture dishes and further cultured. When confluence of cells reached to 80% in the culture dishes, cells were trypsinized and harvested, followed by fixation and permeation, thereafter, stained with propidium iodide using Cell Cycle Phase Determination Kit (Cayman Chemical Co., Ann Arbor, MI) according to the manufacturer's instruction.

Samples were analyzed by flow cytometer (REF 342975, BD FACS Calibur™, BD Biosciences, San Jose, CA) in the FL2 channel with a 488 nm excitation laser. Results were analyzed with Flow Jo software (Tree Star Inc., Pasadena, TX). The proportion of cells in each cell cycle phase was calculated and compared with control.

Xenograft Transplantation of Tumor Cells

NOD.CB17-Prkdc^{scid}/J (NOD-SCID) strains were obtained from Charles River Japan (Yokohama, Japan) and maintained in individual cages on a 12-hr light-dark photocycle, with free access to water and a stock pellet diet (CRF-1, Oriental Yeast, Tokyo, Japan). Stably transfected MCF7 cells were injected subcutaneously into the fourth inguinal mammary fat pad of NOD-SCID mice at a density of 1×10^6 cells in $140 \mu\text{l}$ medium with 50% (vol/vol) matrigel (Matrigel Basement Membrane Matrix Growth Factor Reduced, Corning Inc., NY). Negative control of MCF7 cells carrying empty vector were injected into the right side of the body and stably transfected MCF7 cells with overexpression or knockdown of human KLF15 or PKM2 respectively, were injected into the left side. Tumor growth was monitored by caliper measurement every 6-day in two dimensions. Tumor volumes were calculated using the equation “ $V = (\pi/6) (\text{Length} \times \text{Width}^2)$ ”. After incubation for 31-day, NOD-SCID mice carrying xenograft tumor were sacrificed. Goss morphology and weight of xenografts were

examined.

Immunohistochemical Analysis of Human Breast Tissues

To determine the expression of PKM2 and KLF15 in human breast cancer tissues, 12 specimens of invasive ductal carcinoma of human breast were obtained from Japanese female patients (age: 46-87 years) who underwent surgical treatment in the Department of Surgery, Tohoku University Hospital, Sendai, Japan. All of the patients did not receive chemotherapy, irradiation or hormonal therapy before the surgery. A Histofine Kit (Nichirei, Tokyo, Japan), which employs streptavidin-biotin amplification method, was used. Dilutions of primary antibodies used in this study were as follows: KLF15: 1/200 and PKM2: 1/300. The antigen-antibody complex was visualized with 3,3'-diaminobenzidine (DAB) solution (1mM DAB, 50mM Tris-HCl buffer (pH 7.6), and 0.006% (H₂O₂) and counterstained with hematoxylin.

Statistical Analysis

Statistical analysis was performed using the Student's t test. A *p* value that lower than 0.05 was considered significant (*: *p* < 0.05). Results are the mean±SEM of at least three determinations. In box plot graphs, a box shows one standard deviation above and below the mean of the data, and the median of the data was showed by a line inside the box, whiskers

show the minimum and maximum of all the data. The data in table 10 were evaluated by a crosstabulation analysis using the Chi-square test (an index of association).

Results

1. PKM2 is a novel interacting partner of KLF15

Although KLF15 is suggested to play roles in cancer cell proliferation, the precise molecular mechanism remains unknown. To address this, we started to identify cellular interacting partners of KLF15 in T47D breast cancer cells using in-solution digestion and subsequent shot-gun mass spectrometry. Eleven candidates of KLF15 binding protein (**Table 9**) were identified, including p300 that is known to bind KLF15⁽³⁶⁾. Among others, we decided to focus on PKM2, which is recently highlighted to act as not only a metabolic regulator but also a transcriptional modulator (See Introduction). **Fig. 1** showed the protein profile after immunoprecipitation with anti-Flag antibody and exogenously expressed Flag-tagged KLF15 in C2C12 muscle cells but also in T47D breast cancer cells.

To confirm the interaction between KLF15 and PKM2 in breast cancer cells, immunoprecipitation assay was performed. **Fig. 2** showed that such interaction was observed not only in T47D but also in other breast cancer cell lines, i.e., MDA-MB-231, ZR-75-1, and MCF7, as well as HEK293 human embryonic kidney cells and HepG2 hepatoma cells.

2. KLF15 shows cell type-dependent expression profile

Next, we examined mRNA and protein levels of KLF15 and PKM2. At both mRNA

levels (**Fig. 3A**) and protein levels (**Fig. 3B**), KLF15 showed significant cell-to-cell variation, but PKM2 did less variation. Among those cell lines so far tested, T47D, MCF7 and MDA-MB-231 breast cancer cell lines expressed both factors at various levels.

3. KLF15-PKM2 interaction downregulates β -catenin-dependent reporter gene expression in breast cancer cell

We explored the subcellular localization of both KLF15 and PKM2 in MCF7 cell line and MDA-MB-231 cell line. Immunocytochemistry analysis demonstrated that KLF15 is preferentially expressed in the nucleus, while PKM2 is expressed in both the nucleus and cytoplasm⁽¹⁹⁻²³⁾ (**Fig. 4**).

Next, we performed domain deletion analysis to biochemically confirm the minimal region crucial for the KLF15-PKM2 interaction (See legend for **Fig. 5** for details). The structure and functional domains of mouse KLF15, PKM1 and PKM2 (full-length and deletion mutants) were presented in **Fig. 5A and Fig. 5B**.

Fig. 5C indicated that the deletion of either N-terminal or C-terminal region of KLF15 disturbed its binding with PKM2, and amino acids 1-377 of PKM2 are required for the interaction.

Then we further delineated the interaction domain of KLF15. The structure and

functional domains of human KLF15 (full-length and deletion mutants: D1 to D6) were shown in **Fig. 6A**.

Amino acids 45-351 of KLF15 (D3 and D4), a region spanning β -catenin repression domain and zinc finger 1, were identified as the critical region for the KLF15-PKM2 interaction in MCF7 and MDA-MB-231 cells. Disruption of amino acids 45-351 of KLF15 (D1, D2, D5, and D6) in breast cancer cells abolished the binding between KLF15 and PKM2 as shown in **Fig. 6B**.

As showed in introduction, activation of β -catenin, a crucial signaling pathway for promoting tumor progress, is advanced by nuclear PKM2. Given this, in order to demonstrate the potential function of KLF15 in PKM2-driven β -catenin signaling, we studied the effect of KLF15 and its deletion mutants on PKM2-driven β -catenin-dependent gene expression. Overexpression of PKM2 led to upregulation of β -catenin-dependent gene expression. This effect was abolished by co-expression of KLF15. Moreover, corresponding to the results of domain deletion analysis, KLF15 mutants lacking PKM2 binding (D1, D2, D5, and D6 in **Fig. 6C**) did not show repressive reporter gene expression. In contrast, KLF15-PKM2 interaction domains (D3 and D4) showed similar inhibitory effect as full-length KLF15.

4. PKM2/ β -catenin-downstream factors and cell cycle regulators are inhibited by

KLF15 overexpression in stably transfected MCF7 cells

Since β -catenin is known to accelerate breast cancer cell growth (See Introduction), we established stable cell lines that are genetically engineered to express KLF15 or PKM2 at various levels, to test the effect of KLF15 and PKM2 on breast cancer cell growth.

Expression levels and subcellular localization of exogenous and endogenous proteins in each stably transfected cell lines were shown in **Fig. 7A**. As described above, exogenous KLF15 localized in the nucleus as well as endogenous KLF15. PKM2, either exogenous or endogenous, appeared to be evenly distributed in the cytoplasm and nucleus.

For comparing the expression levels of downstream factors upon manipulation of KLF15 or PKM2 in those engineered cell lines, we determined protein levels of various molecules. Among others, protein levels of PKM2/ β -catenin downstream factors (c-Myc, PTBP1), and KLF15 downstream factors (cell cycle regulators: MCM2 and CDK2) appeared to be reduced in KLF15-overexpressing cells and PKM2-knockdown cells. In contrast, expressions of those proteins appeared to be enhanced when KLF15 was knocked down or PKM2 was over expressed. Moreover, overexpression of KLF15 was accompanied by downregulated PKM2 level, and silencing expression of PKM2 enhanced KLF15 protein level in those engineered cell lines as well. (**Fig. 7B**)

5. Overexpression of KLF15 downregulates cell distribution in G2/M phase, inhibits cell proliferation and migration

Cell cycle distribution of stably transfected cell lines was shown in **Fig. 8A**. Compared with PKM2-overexpressing or KLF15-knockdown cell lines, cells with overexpression of KLF15 showed G0/G1/S phase-dominant cell distribution along with less cell proportion in G2/M phase. Knockdown of PKM2 exhibited the similar effect to overexpression of KLF15. The quantification of cell population in each phase was summarized in **Fig. 8B**.

After incubation for 24 hr, 48 hr and 72 hr respectively, cells with overexpression of KLF15 or knockdown of PKM2 exhibited suppressive proliferation rate, but cells with overexpression of PKM2 or knockdown of KLF15 showed rather increased cell proliferation rate, when compared with wild-type control cells (**Fig. 9A**).

Wound healing assay further supported these tendency. Cells with KLF15-overexpression or PKM2-knockdown showed delayed wound healing after injured for 24 hr and 48 hr; however, cells with PKM2-overexpression or KLF15-knockdown exhibited promoted wound healing during the same period (**Fig. 9B**). The quantification of wound healing rate for each cell line was summarized in **Fig. 9C**.

6. KLF15 suppresses breast cancer cell xenograft growth

In order to determine the effect of KLF15 or PKM2 on breast cancer cell xenograft, we examined xenografted tumor formation and growth using the stable cell lines in NOD-SCID mice. **Fig. 10** represented typical results at 24-day after transplantation of host MCF7 cells and MCF7 cells with either KLF15-overexpression or KLF15-knockdown. MCF7-derived tumor formation was suppressed when KLF15 was over expressed. In contrast, tumor volume was increased when KLF15 was knocked down.

Two dimensions of each tumor were monitored at indicated time point in order to calculate volumes using the equation “ $V = (\pi/6) (\text{Length} \times \text{Width}^2)$ ”. After xenografts were harvested by surgical resection at the 31-day post-cell implantation, weight of each tumor was measured. Typical photographs of isolated tumors were demonstrated in **Fig. 11A**. As shown in **Fig. 11B**, tumor volume appeared to be positively modulated by PKM2 but negatively by KLF15 during 24 days after cell transplantation. As shown in **Fig. 11C**, tumor mass was shown to be downregulated by KLF15-overexpression, but upregulated by PKM2-overexpression at the 31-day post cell implantation.

7. Expressions of KLF15 and PKM2 show an inverse association in human breast carcinoma

We performed immunohistochemical analysis of KLF15 and PKM2 in pathological specimens obtained from patients with breast carcinoma. As in the case with cultured cells, KLF15 predominantly localized in the nucleus, and PKM2 did in both cytoplasm and nucleus (**Fig. 12A**). Although only 12 patient samples were analyzed at this moment, we observed a strong inverse association between the expressions of KLF15 and PKM2. Of the 12 samples, 4 out of 12 (33%) are KLF15+/PKM2-, whereas 6 out of 12 (50%) are PKM2+/KLF15- (**Table 10**).

Moreover, we examined the immunoreactivity of KLF15 and PKM2 in normal mammary gland tissues. KLF15 immunoreactivity was detected in the epithelium of non-neoplastic mammary glands. PKM2 was weakly immunolocalized in some epithelial cells (**Fig. 12B**).

Discussion

In the present study, we investigated the functions of KLF15 in breast cancer cells. We found that KLF15 interacts with PKM2, a tumor promoter. As shown in introduction, PKM2 has a variety of positive actions in breast cancer tumorigenesis, but KLF15 exhibits anti-proliferative effect on T47D breast cancer cells. Given those reports and our results, we hypothesized that KLF15 might be a tumor suppressor, and the effect of KLF15 in cancer biology might be partly mediated by interaction with PKM2.

Stable overexpression and knockdown of KLF15 presented opposite effects on host MCF7 cell growth, suppressive and promotive one, respectively. In support of the previous observations, stable overexpression and knockdown of PKM2 revealed again opposite effect on host MCF7 cell growth, promotive and suppressive one, respectively. The important question is whether this negative effect of KLF15 is mediated via interaction with PKM2. KLF15 has been shown to play roles in cell growth and proliferation. On the other hand, β -catenin signaling is one of the most critical pathways contributing to tumor progress, which has been identified as a novel effector of nuclear PKM2^(19, 22). In this line, studying the effect of KLF15 on β -catenin activity could provide a mechanistic cue for its anti-proliferative action in tumor. In our study, we focused on the effect of KLF15-PKM2 interaction on

β -catenin activity. As shown in **Fig. 6**, repressive effect of KLF15 on PKM2-driven β -catenin-dependent gene expression is suggested to require the interaction domain between KLF15 and PKM2. This observation highlights a crucial role of KLF15-PKM2 interaction in β -catenin signaling pathway. Moreover, in KLF15-overexpressing and PKM2-knockdown MCF7 cells, protein levels of β -catenin downstream factors (c-Myc, PTBP1) appeared to be reduced. It has been reported that both PKM2 and PKM1 arise from same PKM gene through splicing regulation of pre-messenger RNA. In tumors, polypyrimidine track binding protein (PTBP1), a target factor of c-Myc, is one of the major splicing regulators and results in inhibition of PKM1 mRNA splicing along with preferential PKM2 expression ^(19, 22, 47). In KLF15-overexpressing cells, downregulated protein levels of c-Myc and PTBP1 are accompanied by decreased PKM2 level. Our findings, in concert with those of other research groups ⁽³²⁾, indicate the importance of KLF15 in repressing β -catenin activation, and support the idea that KLF15-PKM2 interaction might be one of the molecular mechanisms for KLF15 in regulating breast cancer cell proliferation.

However, the results in **Table 10** raise an important issue that breast cancer might be divided into two categories according to expression levels of KLF15 and PKM2: KLF15-high/PKM2-low and KLF15-low/PKM-high. KLF15-high/PKM2-low tumors might

not require PKM2-mediated process for tumorigenesis, but KLF15-low/PKM2-high tumors might be dependent on PKM2-mediated cellular machinery. It might be intriguing to study this mutually exclusive expression of KLF15 and PKM2.

In cancer biology, the role of PKM2 acting as a promoter of tumorigenesis has been emphasized in two aspects. First, less active dimeric PKM2 is crucial for Warburg effect, and allows tumor cells to synthesize macromolecules (amino acids, phospholipids, and nucleic acids) by using a large fraction of glucose metabolites ⁽¹⁶⁻¹⁸⁾. Second, non-metabolic functions of PKM2 are conducted primarily in the nucleus, correlating with Wnt/ β -catenin ⁽²²⁾, hypoxia-inducible factor 1 α (HIF-1 α) ⁽²⁰⁾, NF- κ B signaling pathway ⁽⁴⁸⁾, as well as phosphoinositide 3-kinase (PI3K)/mammalian target of rapamycin (mTOR) signalling pathway ⁽⁴⁹⁾. However, exceptions are also raised. It has been suggested that PKM2 is not essential for the growth of some tumors. For example, PKM2-knockdown showed no effect on HCT116 colon cancer cell xenograft growth, even though PKM2-knockdown inhibited cell proliferation in cultured cells ⁽⁵⁰⁾. Moreover, xenograft tumors deriving from breast tumor cells with PKM2-knockdown showed the ability of growth as that from PKM2-expressing cells ⁽⁵¹⁾. Analysis of large-scale human tissue proteome via “The Human Protein Atlas” revealed extremely high RNA level of PKM2 in MCF7 cell line, however, PKM2 exhibited

high level in 2 cases, medium level in 6 cases, low level in 2 cases, negative in 2 cases, out of 12 breast cancer patients. The uneven expression of PKM2 in breast cancers can also be observed in our study as showed in **Table 10**. Furthermore, previous investigation demonstrated the existence of loss-of-function mutation, as well as lower enzyme activity mutation of PKM2 in breast cancers ⁽⁵¹⁾. Therefore, further characterization of the biological significance of the KLF15-PKM2 interaction would contribute to clarifying the role of KLF15 and PKM2, as well as the development of a novel therapeutic approach in breast cancer.

Previous investigation reported that KLF15 inhibits estrogen-induced T47D cell proliferation, suggested a role of ER in KLF15 function. But, in the present study, we did not find the correlation between expression of ER and KLF15-PKM2 interaction. In immunoprecipitation experiments, KLF15 was precipitated with PKM2 irrespective of whether the presence of ER or not in breast cancer cells.

Of course, we cannot rule out such possibility that KLF15 acts as a tumor suppressor in PKM2-independent fashion. Indeed, MCF7 cells with KLF15-overexpression exhibited downregulation of MCM2 and CDK2 protein levels. It has been known that decreased expression of MCM2 and CDK2 contributes to decreased cell population in G2/M phase and

suppressive cell proliferation rate^(37, 40). KLF15 also inhibits growth and transformation of human BxPC-3 cells via suppressing the effect of oncogenic KRAS⁽³⁹⁾. Moreover, KLF15 shows the inhibitory effect on NF- κ B signal⁽³²⁾. These findings together with ours imply that the potential anti-proliferative effect of KLF15 might be mediated by diverse ways, which may not limit to via interaction with PKM2.

Conclusion

KLF15 might be a potential breast tumor suppressor. The functions of KLF15 in tumor biology may partly mediate by, but not limits to, the interaction with PKM2 and inhibition of PKM2/ β -catenin/c-Myc/PTBP1 feedback loop signaling network.

References

1. Incidence of breast cancer: World Cancer Report 2014. International Agency for Research on Cancer, World Health Organization. ISBN 978-92-832-0432-9 (2014).
2. Stewart, B. & Wild, C. P. World Cancer Report. ISBN-13 9789283204329 (2014).
3. Eroles, P., Bosch, A., Pérez-Fidalgo, J. A. & Lluch, A. Molecular biology in breast cancer: intrinsic subtypes and signaling pathways. *Cancer Treat. Rev.* 38 (6): 698-707 (2012).
4. Lim, E., Metzger-filho, O. & Winer, E. P. The natural history of hormone receptor-positive breast cancer. *Oncology* 26 (8): 688-694 (2012).
5. Untch, M. & Thomssen, C. Clinical practice decisions in endocrine therapy. *Cancer Invest.* 28 (1): 4-13 (2010).
6. Yu, K. D., Wu, J., Shen, Z. Z. & Shao, Z. M. Hazard of breast cancer-specific mortality among women with estrogen receptor-positive breast cancer after five years from diagnosis: implication for extended endocrine therapy. *J. Clin. Endocr. Metab.* 97 (12): E2201-2209 (2012).
7. Bentzon N., Durning M., Rasmussen B.B., Mouridsen H. & Kroman N. Prognostic effect of estrogen receptor status across age in primary breast cancer. *Int. J. Cancer* 122 (5): 1089-1094 (2008).

8. Hennessy, B. T., Gonzalez-Angulo, A. M., Stemke-Hale, K., Gilcrease, M. Z., Krishnamurthy, S., Lee, J., Fridlyand, J., Sahin, A., Agarwal, R., Joy, C., Liu, W., Stivers, D., Baggerly, K., Carey, M., Lluch, A., Monteagudo, C., He, X., Weigman, V., Fan, C., Palazzo, J., Hortobagyi, G. N., Nolden, L. K., Wang, N. J., Valero, V., Gray, J. W., Perou, C. M. & Mills, G. B. Characterization of a naturally occurring breast cancer subset enriched in epithelial-to-mesenchymal transition and stem cell characteristics. *Cancer Res.* 69 (10): 4116-4124 (2009).
9. Clevers, H. & Nusse, R. Wnt/ β -catenin signaling and disease. *Cell* 149 (6): 1192-1205 (2012).
10. Privette-Vinnedge, L. M., Benight, N. M., Wagh, P. K., Pease, N. A., Nashu, M. A., Serrano-Lopez, J., Adams, A. K., Cancelas, J. A., Waltz, S. E. & Wells, S. I. The DEK oncogene promotes cellular proliferation through paracrine Wnt signaling in Ron receptor-positive breast cancers. *Oncogene* [Epub ahead of print] (2014).
11. Wang, A., Wang, J., Ren, H., Yang, F., Sun, L., Diao, K., Zhao, Z., Song, M., Cui, Z., Wang, E., Wei, M. & Mi, X. TRAF4 participates in Wnt/ β -catenin signaling in breast cancer by upregulating β -catenin and mediating its translocation to the nucleus. *Mol. Cell Biochem.* 395: 211–219 (2014).

12. Rota, L. M., Albanito, L., Shin, M. E., Goyeneche, C. L., Shushanov, S., Gallagher, E. J., LeRoith, D., Lazzarino, D. A. & Wood, T. L. IGF1R inhibition in mammary epithelia promotes canonical Wnt signaling and Wnt1-driven tumors. *Cancer Res.* 74 (19): 201 (2014).
13. Perez-Yepe, E. A., Ayala-Sumuano, J. T., Lezama, R. & Meza, I. A novel β -catenin signaling pathway activated by IL-1 β leads to the onset of epithelial–mesenchymal transition in breast cancer cells. *Cancer Lett.* 354(1): 164-71 (2014).
14. Rostas, J. W., Pruitt, H. C., Metge, B. J., Mitra, A., Bailey, S. K., Bae, S., Singh, K. P., Devine, D. J., Dyess, D. L., Richards, W. O., Tucker, J. A., Shevde, L. A. & Samant, R. S. microRNA-29 negatively regulates EMT regulator N-myc interactor in breast cancer. *Mol. Cancer* 13: 200-210 (2014).
15. Henry, C., Quadir, A., Hawkins, N. J., Jary, E., Llamosas, E., Kumar, D., Daniels, B., Ward, R. L. & Ford, C. E. Expression of the novel Wnt receptor ROR2 is increased in breast cancer and may regulate both β -catenin dependent and independent Wnt signaling. *J. Cancer Res. Clin.* [Epub ahead of print] (2014).
16. Koppenol, W. H., Bounds, P. L. & Dang, C.V. Otto Warburg's contributions to current concepts of cancer metabolism. *Nat. Rev. Cancer* 11(5): 325-337 (2011).

17. Christofk, H. R., Heiden, M. G. V., Harris, M. H., Ramanathan, A., Gerszten, R. E., Wei, R., Fleming, M. D., Schreiber, S. L. & Cantley, L. C. The M2 splice isoform of pyruvate kinase is important for cancer metabolism and tumour growth. *Nature* 452: 230-234 (2008).
18. Chaneton, B., Hillmann, P., Zheng, L., Martin, A. C. L., Maddocks, O. D. K., Chokkathukalam, A., Coyle, J. E., Jankevics, A., Holding, F. P., Vousden, K. H., Frezza, C., O'Reilly, M. & Gottlieb, E. Serine is a natural ligand and allosteric activator of pyruvate kinase M2. *Nature* 491: 458–462 (2012).
19. Yang, W., Zheng, W., Xia, Y., Ji, H., Chen, X., Guo, F., Lyssiotis, C. A., Aldape, K., Cantley, L. C. & Lu, Z. ERK1/2-dependent phosphorylation and nuclear translocation of PKM2 promotes the Warburg effect. *Nat. Cell Biol.* 14: 1295-1304 (2012).
20. Luo, W., Hu, H., Chang, R., Zhong, J., Knabel, M., O'Meally, R., Cole, R. N., Pandey, A. & Semenza, G. L. Pyruvate kinase M2 is a PHD3-stimulated coactivator for hypoxia-inducible factor1. *Cell* 145: 732-744 (2011).
21. Gao, X., Wang, H., Jenny, J. Y., Liu, X. & Liu, Z. R. Pyruvate kinase M2 regulates gene transcription by acting as a protein kinase. *Mol. Cell* 45: 598-609 (2012).
22. Yang, W., Xia, W., Ji, H., Zheng, Y., Liang, J., Huang, W., Gao, X., Aldape, K. & Lu, Z.

- Nuclear PKM2 regulates β -catenin transactivation upon EGFR activation. *Nature* 480:118-122 (2011).
23. Wang, H. J., Hsieh, Y. J., Cheng, W. C., Lin, C. P., Lin, Y. S., Yang, S. F., Chen, C. C., Izumiya, Y., Yu, J. S., Kung, H. J. & Wang, W. C. JMJD5 regulates PKM2 nuclear translocation and reprograms HIF-1 α -mediated glucose metabolism. *Proc. Natl Acad. Sci. USA*. 111 (1): 279-284 (2014).
24. Shimada, N., Shinagawa, T. & Ishii S. Modulation of M2-type pyruvate kinase activity by the cytoplasmic PML tumor suppressor protein. *Genes Cells* 13: 245–254 (2008).
25. Shashni, B., Sakharkar, K. R., Nagasaki, Y. & Sakharkar, M. K. Glycolytic enzymes PGK1 and PKM2 as novel transcriptional targets of PPAR γ in breast cancer pathophysiology. *J. Drug Target*. 21 (2): 161–174 (2013).
26. He, X., Arslan, A. D., Ho, T., Yuan, C., Stampfer, M. R. & Beck, W. T. Involvement of polypyrimidine tract-binding protein (PTBP1) in maintaining breast cancer cell growth and malignant properties. *Oncogenesis* 3: e84-e91 (2014).
27. Bonuccelli, G., Whitaker-Menezes, D., Castello-Cros, R., Pavlides, S., Pestell, R. G., Fatatis, A., Witkiewicz, A. K., Heiden, M. G. V., Migneco, G., Chiavarina, B., Frank, P. G., Capozza, F., Flomenberg, N., Martinez-outschoorn, U. E., Sotgia, F. & Lisanti, M. P. The

- reverse Warburg effect: Glycolysis inhibitors prevent the tumor promoting effects of caveolin-1 deficient cancer associated fibroblasts. *Cell Cycle* 9 (10): 1960-1971 (2010).
28. Chiavarina, B., Whitaker-Menezes, D., Martinez-Outschoorn, U. E., Witkiewicz, A. K., Birbe, R. C., Howell, A., Pestell, R. G., Smith, J., Daniel, R., Sotgia, F. & Lisanti, M. P. Pyruvate kinase expression (PKM1 and PKM2) in cancer-associated fibroblasts drives stromal nutrient production and tumor growth. *Cancer Biol. Ther.* 12 (12): 1101–1113 (2011).
29. Li, W., Liu, J., Jackson, K., Shi, R. & Zhao, Y. Sensitizing the therapeutic efficacy of taxol with Shikonin in human breast cancer cells. *Plos One* 9 (4): e94079 (2014).
30. Uchida, S., Tanaka, Y., Ito, H., Saitoh-ohara, F., Inazawa, J., Yokoyama, K. K., Sasaki, S. & Marumo, F. Transcriptional regulation of the CLC-K1 promoter by myc-associated zinc finger protein and kidney-enriched Krüppel-Like Factor, a novel zinc finger repressor. *Mol. Cell. Biol.* 20: 7319–7331 (2000).
31. Mas, C., Lussier-Price, M., Soni, S., Morse, T., Arseneault, G., Lello, P. D., Lafrance-Vanasse, J., Bieker, J. J. & Omichinski, J. G. Structural and functional characterization of an atypical activation domain in erythroid Krüppel-like factor (EKLF). *Proc. Natl Acad. Sci. USA.* 108 (26): 10484-10489 (2011).

32. Noack, C., Zafiriou, M. P., Schaeffer, H. J., Renger, A., Pavlova, E., Dietz, R., Zimmermann, W. H., Bergmann, M. W. & Zelarayán, L. C. Krueppel-like factor 15 regulates Wnt/ β -catenin transcription and controls cardiac progenitor cell fate in the postnatal heart. *EMBO Mol. Med.* 4: 992–1007 (2012).
33. Haldar, S. M., Jeyaraj, D., Anand, P., Zhu, H., Lu, Y., Prosdocimo, D. A., Eapen, B., Kawanami, D., Okutsu, M., Brotto, L., Fujioka, H., Kerner, J., Rosca, M. G., McGuinness, O. P., Snow, R. J., Russell, A. P., Gerber, A. N., Bai, X., Yan, Z., Nosek, T. M., Brotto, M., Hoppel, C. L. & Jain, M. K. Kruppel-like factor 15 regulates skeletal muscle lipid flux and exercise adaptation. *Proc. Natl Acad. Sci. USA.* 109: 6739–6744 (2012).
34. Haldar, S. M., Lu, Y., Jeyaraj, D., Kawanami, D., Cui, Y., Eapen, S. J., Hao, C., Li, Y., Doughman, Y. Q., Watanabe, M., Shimizu, K., Kuivaniemi, H., Sadoshima, J., Margulies, K. B., Cappola, T. P. & Jain, M. K. KLF15 deficiency is a molecular link between heart failure and aortic aneurysm formation. *Sci. Transl. Med.* 2 (26): 26ra26 (2010).
35. Leenders, J. J., Wijnen, W. J., Made, I., Hiller, M., Swinnen, M., Vandendriessche, T., Chuah, M., Pinto, Y. M. & Creemers, E. E. Repression of cardiac hypertrophy by KLF15: underlying mechanisms and therapeutic implications. *Plos One* 7 (5): e36754 (2012).
36. Lu, Y., Zhang, L., Liao, X., Sangwung, P., Prosdocimo, D. A., Zhou, G., Votruba, A. R.,

- Brian, L., Han, Y. J., Gao, H., Wang, Y., Shimizu, K., Weinert-Stein, K., Khrestian, M., Simon, D. I., Freedman, N. J. & Jain, M. K. Kruppel-like factor 15 is critical for vascular inflammation. *J. Clin. Invest.* 123 (10): 4232–4241 (2013).
37. Hong, Q., Li, C., Xie, Y., Lv, Y., Liu, X., Shi, S., Ding, R., Zhang, X., Zhang, L., Liu, S. & Chen, X. Kruppel-like Factor-15 inhibits the proliferation of mesangial cells. *Cell. Physiol. Biochem.* 29: 893-904 (2012).
38. Masuno, K., Haldar, S. M., Jeyaraj, D., Mailloux, C. M., Huang, X., Panettieri Jr, R. A., Jain, M. K. & Gerber, A. N. Expression profiling identifies Klf15 as a glucocorticoid target that regulates airway hyperresponsiveness. *Am. J. Resp. Cell Mol. Biol.* 45: 642–649 (2011).
39. Fernandez-Zapico, M. E., Lomberk, G. A., Tsuji, S., Demars, C. J., Bardsley, M. R., Lin, Y. H., Almada, L. L., Han, J. J., Mukhopadhyay, D., Ordog, T., Buttar, N. S. & Urrutia, R. A functional family-wide screening of SP/KLF proteins identifies a subset of suppressors of KRAS-mediated cell growth. *Biochem. J.* 435: 529–537 (2011).
40. Ray, S. & Pollard, J. W. KLF15 negatively regulates estrogen-induced epithelial cell proliferation by inhibition of DNA replication licensing. *Proc. Natl Acad. Sci. USA.* 109 (21): E1334–E1343 (2012).

41. Yoshikawa, N., Shimizu, N., Sano, M., Ohnuma, K., Iwata, S., Hosono, O., Fukuda, K., Morimoto, C. & Tanaka, H. Role of the hinge region of glucocorticoid receptor for HEXIM1-mediated transcriptional repression. *Biochem. Biophys. Res. Commun.* 371 (1): 44-49 (2008).
42. Miyagishi, M., Fujii, R., Hatta, M., Yoshida, E., Araya, N., Nagafuchi, A., Ishihara, S., Nakajima, T. & Fukamizu, A. Regulation of Lef-mediated transcription and p53-dependent pathway by associating beta-catenin with CBP/p300. *J. Biol. Chem.* 275 (45): 35170-3175 (2000).
43. Dignam, J. D., Lebovitz, R. M. & Roeder, R. G. Accurate transcription initiation by RNA polymerase II in a soluble extract from isolated mammalian nuclei. *Nucleic Acids Res.* 11 (5): 1475-89 (1983).
44. Yoshikawa, N., Nagasaki, M., Sano, M., Tokudome, S., Ueno, K., Shimizu, N., Imoto, S., Miyano, S., Suematsu, M., Fukuda, K., Morimoto, C. & Tanaka, H. Ligand-based gene expression profiling reveals novel roles of glucocorticoid receptor in cardiac metabolism. *Am. J. Physiol-Endoc. M.* 296: E1363-E1373 (2009).
45. Dong, C., Wu, Y., Yao, J., Wang, Y., Yu, Y., Rychahou, P. G., Evers, B. M. & Zhou, B. P. G9a interacts with Snail and is critical for Snail-mediated E-cadherin repression in human

- breast cancer. *J. Clin. Invest.* 122 (4): 1469-1486 (2012).
46. Yu, Z., Wang, L., Wang, C., Ju, X., Wang, M., Chen, K., Loro, E., Li, Z., Zhang, Y., Wu, K., Casimiro, M. C., Gormley, M., Ertel, A., Fortina, P., Chen, Y., Tozeren, A., Liu, Z. & Pestell, R. G. Cyclin D1 induction of Dicer governs microRNA processing and expression in breast cancer. *Nat. Commun.* 4:2812-2811 (2013).
47. David, C. J., Chen, M., Assanah, M., Canoll, P. & Manley, J. L. HnRNP proteins controlled by c-Myc deregulate pyruvate kinase mRNA splicing in cancer. *Nature* 463: 364-368 (2010).
48. Yang, W., Xia, Y., Cao, Y., Zheng, Y., Bu, W., Zhang, L., You, M. J., Koh, M. W., Cote, G., Aldape, K., Li, Y., Verma, I. M., Chiao, P. J. & Lu, Z. EGFR-Induced and PKC ϵ Monoubiquitylation-dependent NF- κ B activation upregulates PKM2 expression and promotes tumorigenesis. *Mol. Cell* 48: 771-784 (2012).
49. Nemazany, I., Espeillac, C., Pende M. & Panasyuk, G. Role of PI3K, mTOR and Akt2 signalling in hepatic tumorigenesis via the control of PKM2 expression. *Biochem. Soc. T.* 41: 917-922 (2013).
50. Cortés-Cros, M., Hemmerlin, C., Ferretti, S., Zhang, J., Gounarides, J. S., Yin, H., Muller, A., Haberkorn, A., Chene, P., Sellers, W. R. & Hofmann, F. M2 isoform of pyruvate kinase

is dispensable for tumor maintenance and growth. *Proc. Natl. Acad. Sci. USA.* 110 (2): 489-494 (2013).

51. Israelsen, W. J., Dayton, T. L., Davidson, S. M., Fiske, B. P., Hosios, A. M., Bellinger, G., Li, J., Yu, Y., Sasaki, M., Horner, J. W., Burga, L. N., Xie, J., Jurczak, M. J., DePinho, R. A., Clish, C. B., Jacks, T., Kibbey, R. G., Wulf, G. M., Vizio, D. D., Mills, G. B., Cantley, L. C. & Vander Heiden, M. G. PKM2 isoform-specific deletion reveals a differential requirement for pyruvate kinase in tumor cells. *Cell* 155: 397-409 (2013).

Table 1. Features of Molecular Subtypes of Breast Cancer

Molecular Subtype	Frequency	ER/PRg/HER2	CK5/6 EGFR	Genes of Proliferation	Histologic Grade	TP53 Mutations	Prognostic
Luminal A	50-60%	ER+ PRg- HER2-	-	Low	Low	Low	Excellent
Luminal B	10-20%	ER+/- PRg+/- HER2-/+	-	High	Intermediate /High	Intermediate	Intermediate/ Bad
Basal-like	10-20%	ER- PRg- HER2-	+	High	High	High	Bad
HER2-enriched	10-15%	ER- PRg- HER2+	+/-	High	High	High	Bad
Normal breast-like	5-10%	ER-/+ HER2-	+	Low	Low	Low	Intermediate
Claudin-low	12-14%	ER- PRg- HER2-	+/-	High	High	High	Bad

Ref. 3 Eroles, P., Bosch, A., Pérez-Fidalgo, J. A. & Lluch, A. Molecular biology in breast cancer: intrinsic subtypes and signaling pathways. *Cancer Treat. Rev.* 38 (6): 698-707 (2012).

Table 2. Reasonable Recommendations – Personalizing the Treatment of Women with Early Breast Cancer: 13th St Gallen 2013

Intrinsic Subtype	ER/PRg/HER2/Ki-67	Notes
Luminal A	Luminal A-like ER+, HER2-, Ki-67 low, PgR high	Interlab variability of Ki67. Added value of PgR in distinguishing between ‘Luminal A-like’ and ‘Luminal B-like’ subtypes (cut-point of 20% or higher to define PgR high).
Luminal B	Luminal B-like (HER2 positive), ER positive, HER2 over-expressed or amplified, any Ki-67 and PgR	Either a high Ki-67 or a low PgR may be used to distinguish between ‘Luminal A-like’ and ‘Luminal B-like’ (HER2 negative).
Erb-B2 overexpression	HER2 positive (non luminal), HER2 over-expressed or amplified ER and PgR absent	The majority of HER2 positive tumors are endocrine-receptor negative.
Basal-like	Triple negative (ductal), ER and PgR absent, HER2 negative	There is approximately an 80% overlap between ‘triple negative’ and intrinsic ‘basal-like’ subtype.

Table 3. Reasonable Recommendations – Personalizing the Treatment of Women with Early Breast Cancer: 13th St Gallen 2013

Subtype	Type of therapy	Notes
Luminal A like	Endocrine therapy alone	Few require cytotoxics
Luminal B like (HER2 negative)	Endocrine therapy for all patients, Cytotoxic therapy for most	Inclusion and type of cytotoxics may depend on level of endocrine receptor expression, perceived risk and patient preference.
Luminal B-like (HER2 positive)	Cytotoxics + anti-HER2 + endocrine therapy	No data are available to support the omission of cytotoxics in this group.
HER2 positive (non luminal)	Cytotoxics + anti-HER2	
Triple negative (ductal)	Cytotoxics	Consider DNA disrupting agents.
Special histological types		
A. Endocrine responsive	Endocrine therapy	Medullary and adenoid cystic carcinomas may not require
B. Endocrine non responsive	Cytotoxics	any adjuvant cytotoxics

13th St Gallen International Breast Cancer Conference, 2013

Table 4. List of Plasmids

NO.	Constructed Plasmids
1	p3×Flag-CMV10-hKLF15
2	p3×Flag-CMV10-hPKM2
3	pFlag-CMX-hKLF15
4	pFlag-CMX-hPKM2
5	pFlag-CMX-mPKM1
6	pFlag-CMX-mPKM2 1aa-306aa
7	pFlag-CMX-mPKM2 1aa-377aa
8	pFlag-CMX-mPKM2 307aa-531aa
9	pFlag-CMX-mPKM2 378aa-433aa
10	pFlag-CMX-mPKM2 378aa-531aa
11	pFlag-CMX-mKLF15 1aa-415aa
12	pHA-CMX-mKLF15 1aa-415aa
13	pHA-CMX-mKLF15 1aa-319aa
14	pHA-CMX-mKLF15 320aa-415aa
15	pEF-BH (β -catenin)
NO.	short hairpin RNA plasmids
1	psilencer-shRNA-hKLF15
2	psilencer-shRNA-hPKM2
NO.	Luciferase Reporter Plasmid
1	TOP-Flash (TCF-WT-LUC)
2	FOP-Flash (TCF-MT-LUC)

Table 5. Oligonucleotide DNA Template and Insert Enzyme Sites for short hairpin RNA (shRNA) Plasmid

shRNA-hKLF15 target sequence: AGGAGAACAUGGAGCCUGGAGUCAA
shRNA-hPKM2 target sequence: GCATCTACCACTTGCAATTA
shRNA template of hPKM2 BamHI/HindIII 5->3
GATCCGCATCTACCACTTGCAATTATTCAAGAGATAATTGCAAGTGGTAGA TGTTTTTTGGAAA
shRNA template of hPKM2 HindIII/BamHI 5->3
AGCTTTTCCAAAAACATCTACCACTTGCAATTATCTCTTGAATAATTGCAA GTGGTAGATGCG
shRNA template of hKLF15 BamHI/HindIII 5->3
GATCCAGGAGAACATGGAGCCTGGAGTCAATTCAAGAGATTGACTCCAGGC TCCATGTTCTCCTTTTTTTGGAAA
shRNA template of hKLF15 HindIII/BamHI 5->3
AGCTTTTCCAAAAAAGGAGAACATGGAGCCTGGAGTCAATCTCTTGAATT GACTCCAGGCTCCATGTTCTCCTG

Oligonucleotides were ordered from Nihon Gene Research Laboratories.

Table 6. Primers and Insert Enzyme Sites for Expression Plasmid (1)

p3×Flag-CMV10-hKLF15 1aa-416aa

CTTGCGGCCGCGAATTCAGtggaccacttacttccagt (EcoRI-5'→3' sense)

GGATGCCACCCGGGATCCTCAgttcacggagcgcacg (BamHI-5'→3' antisense)

p3×Flag-CMV10-hPKM2 1aa-531aa

CTTGCGGCCGCGAATTCAtcgaagccccatagtgaagc (EcoRI-5'→3' sense)

GGATGCCACCCGGGATCCTCAcggcacaggaacaacac (BamHI-5'→3' antisense)

p3×Flag-CMV10-hKLF15 Domain 1aa-205aa

CTTGCGGCCGCGAATTCAGtggaccacttacttccagt (EcoRI-5'→3' sense)

GGATGCCACCCGGGATCCTCActgggcacctctgcact (BamHI-5'→3' antisense)

p3×Flag-CMV10-hKLF15 Domain 1aa-315aa

CTTGCGGCCGCGAATTCAGtggaccacttacttccagt (EcoRI-5'→3' sense)

GGATGCCACCCGGGATCCTCAtgcggtgggttcttggg (BamHI-5'→3' antisense)

p3×Flag-CMV10-hKLF15 Domain 1aa-351aa

CTTGCGGCCGCGAATTCAGtggaccacttacttccagt (EcoRI-5'→3' sense)

GGATGCCACCCGGGATCCTCAgaagggtcttcaccctgt (BamHI-5'→3' antisense)

p3×Flag-CMV10-hKLF15 Domain 45aa-416aa

CTTGCGGCCGCGAATTCAtgcctccagcccctgt (EcoRI-5'→3' sense)

GGATGCCACCCGGGATCCTCAgttcacggagcgcacg (BamHI-5'→3' antisense)

p3×Flag-CMV10-hKLF15 Domain 153aa-416aa

CTTGCGGCCGCGAATTCAGgagcctggagtcaagga (EcoRI-5'→3' sense)

GGATGCCACCCGGGATCCTCAgttcacggagcgcacg (BamHI-5'→3' antisense)

p3×Flag-CMV10-hKLF15 Domain 199aa-416aa

CTTGCGGCCGCGAATTCAcagtgcaggaggtgccca (EcoRI-5'→3' sense)

GGATGCCACCCGGGATCCTCAgttcacggagcgcacg (BamHI-5'→3' antisense)

pFlag-CMX-mPKM1 (mouse brain cDNA) (1aa-531aa)

TTCTAGGTACCAGATATCAccgaagccacacagtgaag (EcoRV-5'→3' sense)

GCTAGCTGGCCAGGATCCTCAaggtacaggcactacacgc (BamHI-5'→3' antisense)

pHA/Flag-CMX-mPKM2 (C2C12 cDNA) (1aa-531aa)

TTCTAGGTACCAGATATCAccgaagccacacagtgaag (EcoRV-5'→3' sense)

GCTAGCTGGCCAGGATCCTCAaggtacaggcactacacgc (BamHI-5'→3' antisense)

Table 6. Primers and Insert Enzyme Sites for Expression Plasmid (2)

pHA/Flag-CMX-mPKM2 Domain 1aa-306aa
TTCTAGGTACCAGATATCAccgaagccacacagtgaag (EcoRV-5'->3' sense)
GCTAGCTGGCCAGGATCCTCAgaccttctctgcaggaa (BamHI-5'->3' antisense)
pHA/Flag-CMX-mPKM2 Domain 1aa-377aa
TTCTAGGTACCAGATATCAccgaagccacacagtgaag (EcoRV-5'->3' sense)
GCTAGCTGGCCAGGATCCTCAggcagcctctgcctc (BamHI-5'->3' antisense)
pHA/Flag-CMX-mPKM2 Domain 307aa-531aa
TTCTAGGTACCAGATATCAAttctggctcagaagatgatg (EcoRV-5'->3' sense)
GCTAGCTGGCCAGGATCCTCAaggtacaggcactacacgc (BamHI-5'->3' antisense)
pHA/Flag-CMX-mPKM2 Domain 378aa-434aa
TTCTAGGTACCAGATATCAatctaccactgcagctattc (EcoRV-5'->3' sense)
GCTAGCTGGCCAGGATCCTCActtggtgagcagataat (BamHI-5'->3' antisense)
pHA/Flag-CMX-mPKM2 Domain 378aa-531aa
TTCTAGGTACCAGATATCAatctaccactgcagctattc (EcoRV-5'->3' sense)
GCTAGCTGGCCAGGATCCTCAaggtacaggcactacacgc (BamHI-5'->3' antisense)
pHA/Flag-CMX-mKLF15 1aa-415aa
TTCTAGGTACCAGATATCAgtggaccacctgcttcag (EcoRV-5'->3' sense)
GCTAGCTGGCCAGGATCCTCAgttgatggcgcgtactg (BamHI-5'->3' antisense)
pHA-CMX-mKLF15 Domain 1aa-319aa
TTCTAGGTACCAGATATCAgtggaccacctgcttcag (EcoRV-5'->3' sense)
TCTAGCTACCTAGCTAGCTCAgtcttggtgtacatctt (NheI-5'->3' antisense)
pHA-CMX-mKLF15 Domain 320aa-415aa
TTCTAGGTACCAGATATCAagccacctcaaggccac (EcoRV-5'->3' sense)
GCTAGCTGGCCAGGATCCTCAgttgatggcgcgtactg (BamHI-5'->3' antisense)
pHA/Flag-CMX-hKLF15 (1aa-416aa)
TTCTAGGTACCAGATATCAgctggaccacttacttcagt (EcoRV-5'->3' sense)
GCTAGCTGGCCAGGATCCTCAgttcacggagcgcacg (BamHI-5'->3' antisense)

Primers were ordered from Nihon Gene Research Laboratories.

Table 7. Primers for DNA Sequencing

p3×Flag-CMV10-EcoRI-hKLF15	
(136s)	CTTGCGGCCGCGAATTCAGCCTCCAGCCCCTGCTC
(457s)	CTTGCGGCCGCGAATTCAGAGCCTGGAGTCAAGGAGG
(781s)	CTTGCGGCCGCGAATTCAGCACTCGTGCCCCAGGTG
(304s)	CTTGCGGCCGCGAATTCACCCGTGGCCTGGGGGC
(595s)	CTTGCGGCCGCGAATTCAGCCAGTGCAGGAGGTGCC
(922s)	CTTGCGGCCGCGAATTCAAAGTTCCCCAAGAACCCAGC
p3×Flag-CMV10-BamHI-hKLF15	
(945a)	GGATGCCACCCGGGATCCTCATGCGGCTGGGTTCTTGGG
(1053a)	GGATGCCACCCGGGATCCTCAGAAGGGCTTCTCACCCGTG
(615a)	GGATGCCACCCGGGATCCTCACTGGGCACCTCCTGCACT
hKLF15 480s	AGTGGCCCCGTGGCCTG
hKLF15 783s	GCAGGAGGTGCCAGGG
hKLF15 1082s	TGCCGGTCTCCTCATGGG
hKLF15 1383s	AAGGTGCACCGCTTCCCG
p3×Flag-CMV10	TCGTTTAGTGAACCGTCAGAA
pHA-CMX 600s	ACTAGAGAACCCACTGCTTAA
mKLF15 ORF 400s	AGGCCCTTCCAGCCTACC
mKLF15 ORF 798s	ACCATCCTCCAACCTGAACC

Primers were ordered from Nihon Gene Research Laboratories.

Table 8. Primers for qRT-PCR (Human)

Target gene	Forward primer (FW)	Reverse primer (RW)
hKLF15:	CAAAAGCAGCCACCTCAAG	TCAGAGCGCGAGAACCTC
hPKM2 #1	TCCGGATCTCTTCGTCTTTG	GTCTGAATGAAGGCAGTCCC
hPKM2 #2	GTCTGGAGAAACAGCCAAGG	CGGAGTTCCTCGAATAGCTG
h β -actin	ATGGATGACGATATCGCTGCGC	GCAGCACAGGGTGCTCCTCA

Primers were ordered from Nihon Gene Research Laboratories.

Table 9. Candidates of KLF15 Interacting Partner

NO.	Protein Candidates	Predicted Molecular Weight
1	Plectin	531kDa
2	Serine/arginine repetitive matrix protein 2	300kDa
3	histone acetyltransferase p300	300kDa
4	spectrin β II	275 kDa
5	carbamoyl phosphate synthetase 2	243kDa
6	Myosin heavy chain	230kDa
7	Pre-lamine A/C	65~80kDa
8	Pyruvate kinase muscle isozyme	58kDa
9	Cpsf7 isoform 1, 2	52kDa
10	Actin(alpha, beta, gamma, kappa)	42~47kDa
11	Tropomyosin alpha-1 chain	33kDa

Table 10. Association between immunohistochemical KLF15 and PKM2 status in human breast carcinoma

		PKM2		<i>p</i> value
		+	-	
KLF15	+	0	4	0.014
	-	6	2	

Values represent the number of cases.

The number of KLF15- and PKM2-positive breast carcinomas were 4 out of 12 (33%) and 6 out of 12 (50%) cases, respectively. An inverse association was detected between KLF15 and PKM2 immunoreactivity in this study.

Figure 1

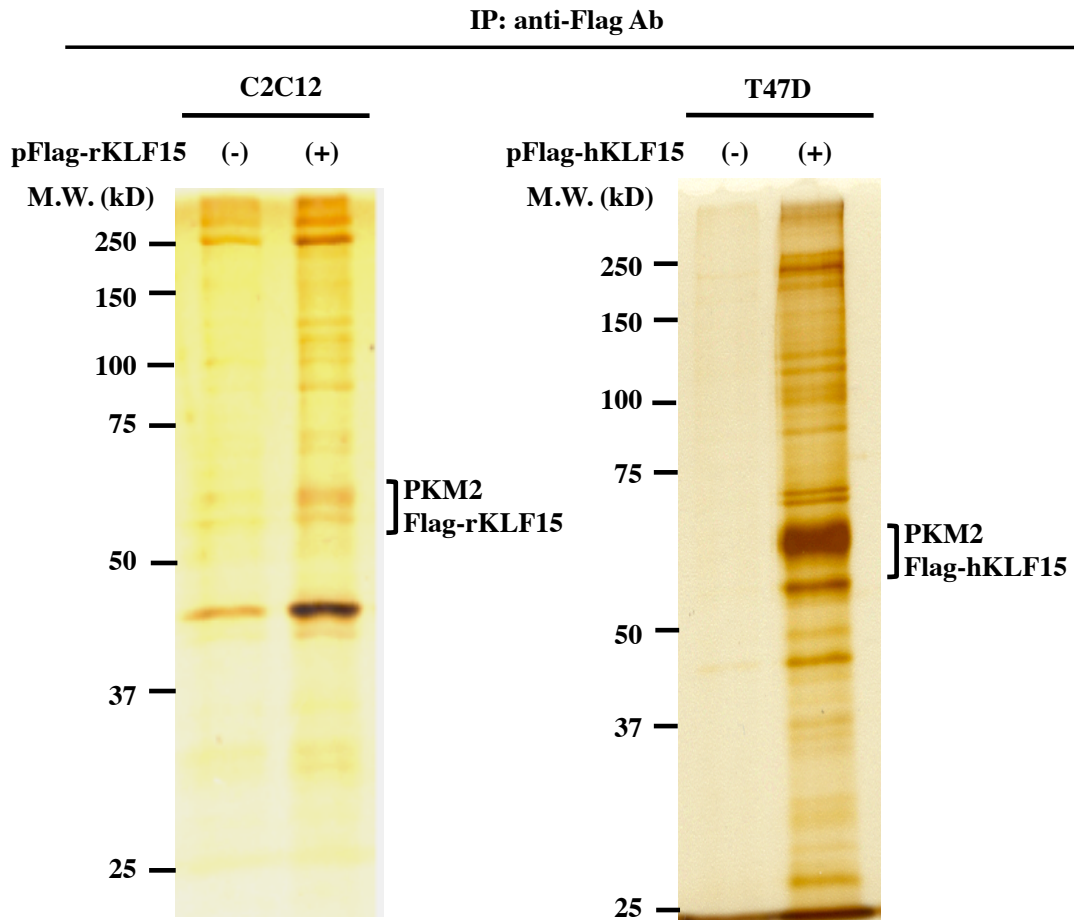


Figure 1. PKM2 is a candidate of KLF15-interacting partners

Nuclear extracts from Flag-tagged rat KLF15 overexpressing C2C12 mouse myoblasts and Flag-tagged human KLF15 overexpressing T47D human breast cancer cells were immunoprecipitated with anti-Flag beads and eluted with Flag peptides. The eluates were resolved by SDS-PAGE, visualized by silver staining, and representative images are shown. IP: Immunoprecipitation; Ab: antibody; M.W.: molecular weight.

Figure 2

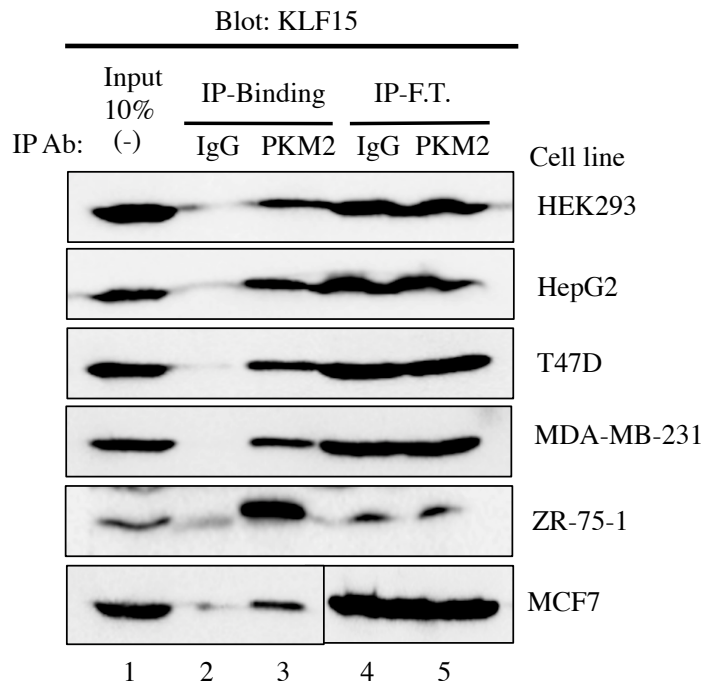
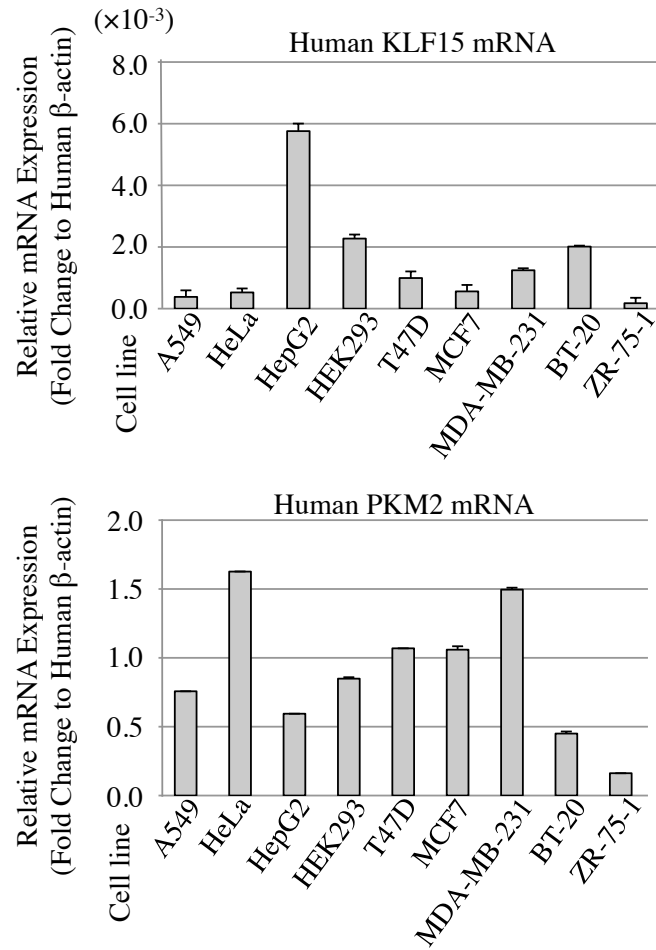


Figure 2. KLF15 interacts with PKM2 in human breast cancer cells.

Whole cell extracts from human embryonic kidney (HEK293), hepatocellular carcinoma (HepG2), and breast cancer (T47D, MDA-MB-231, ZR-75-1, and MCF7) cells were immunoprecipitated with anti-PKM2 antibodies or normal control IgG and were eluted. Ten percent input, eluates, and flow through fractions were separated with SDS-PAGE followed by Western blotting analysis with anti-KLF15 antibodies and representative images from three independent experiments are shown. IP: immunoprecipitation; F.T.: flow through.

Figure 3

A



B

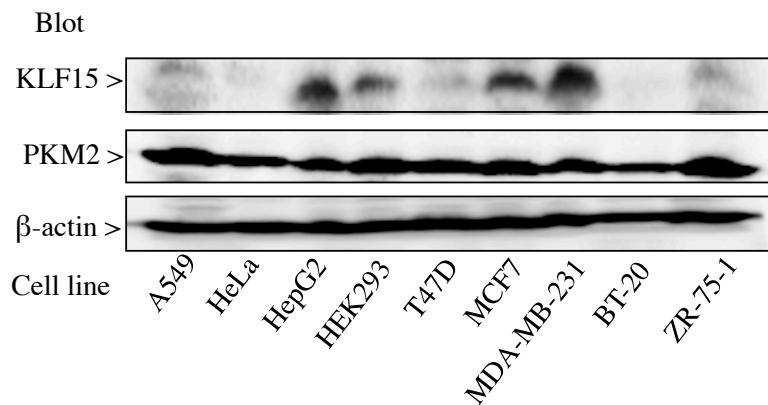


Figure 3. mRNA and protein expression profiles of KLF15 and PKM2 in various human cell lines

- (A) mRNA expression levels of KLF15 and PKM2 in various human cell lines. Total RNA was isolated from indicated cells and mRNA expression levels of KLF15 and PKM2 were analysed by qRT-PCR as described in Materials and Methods. mRNA expression levels are shown as relative mRNA expression levels normalized to β -actin. Data represent the means \pm SEM of three independent experiments.
- (B) Protein expression of KLF15 and PKM2 in various human cell lines. Whole cell extracts were subjected to western blotting analysis with anti-KLF15, PKM2, and β -actin antibodies, respectively. Representative images from three independent experiments are shown.

Figure 4

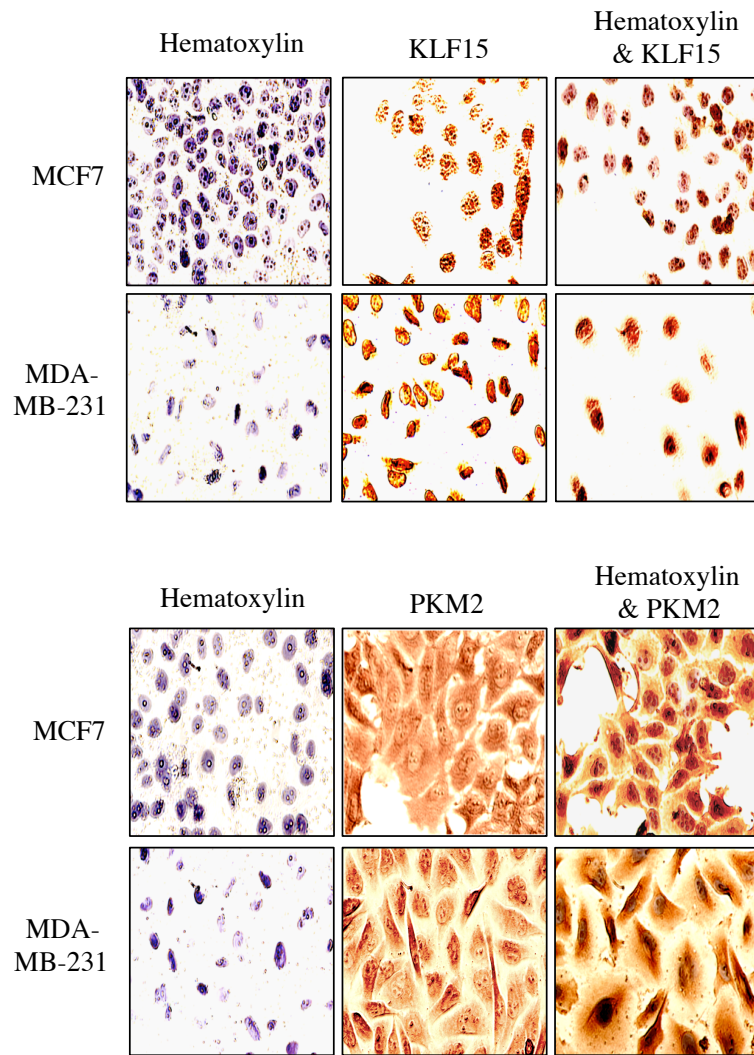


Figure 4. Subcellular localization of KLF15 and PKM2 in human breast cancer cells

Subcellular localization of KLF15 (upper panels) and PKM2 (lower panels) in MCF7 and MDA-MB-231 cells were analyzed with anti-KLF15 (1:100) or PKM2 (1:100) antibodies, indicated by brown staining, and the nucleus was counterstained with hematoxylin. Representative images from three independent experiments are shown. Magnification: 40 \times .

Figure 5

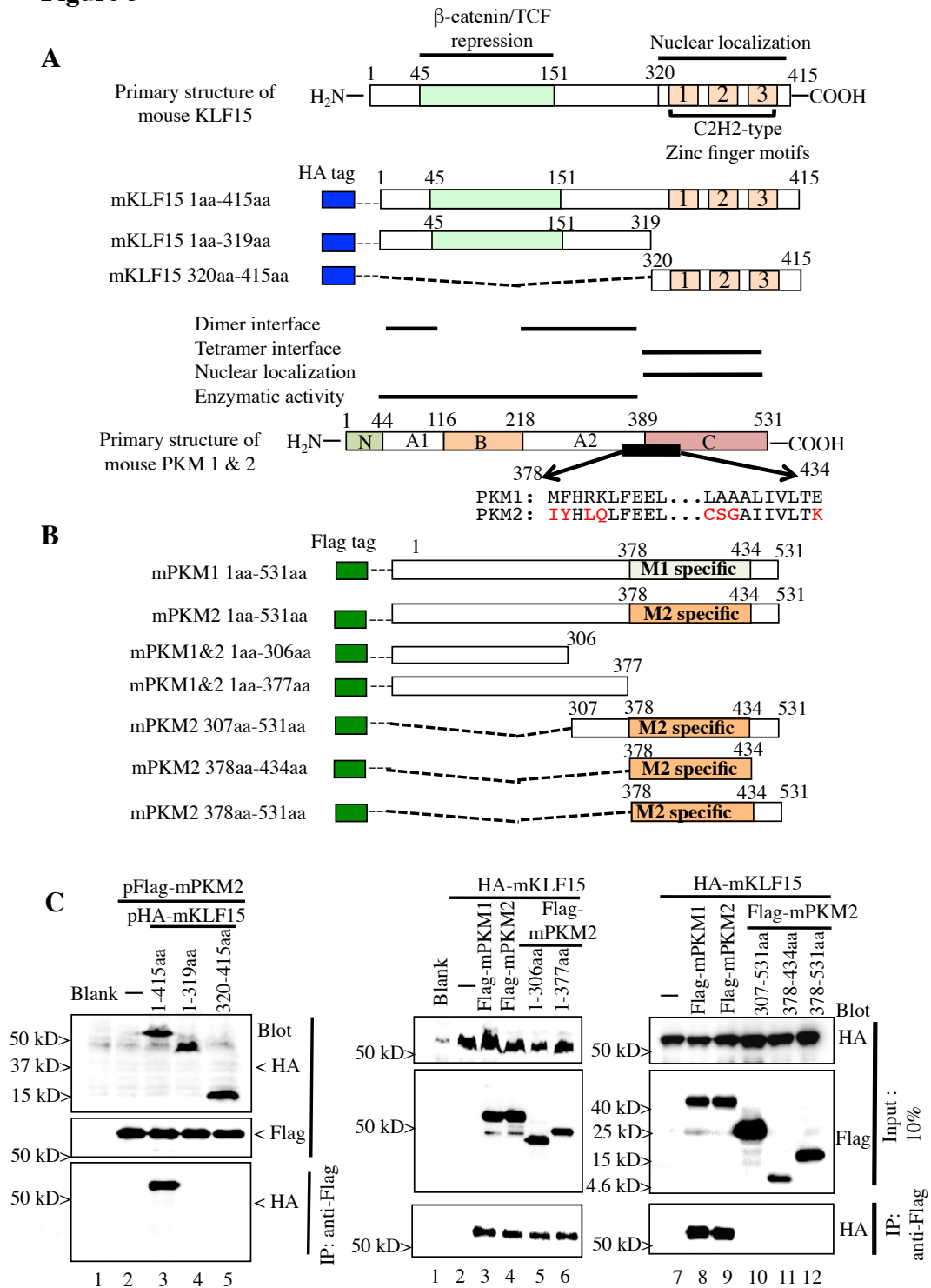
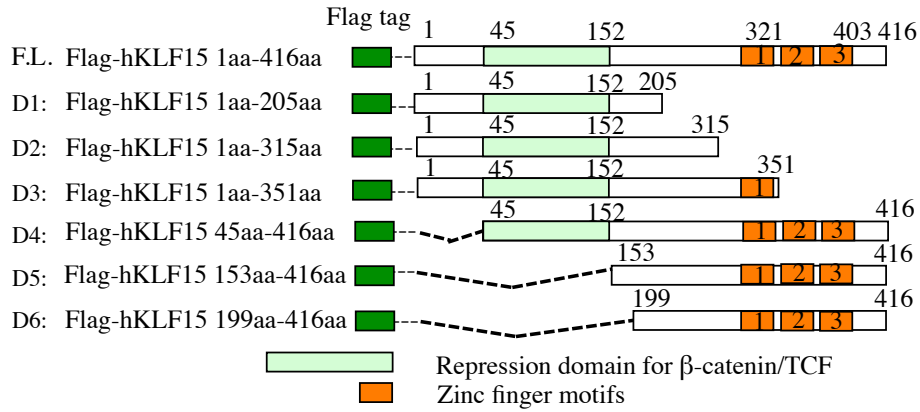


Figure 5. KLF15 interacts with N-terminal region (amino acids 1-377) of PKM2

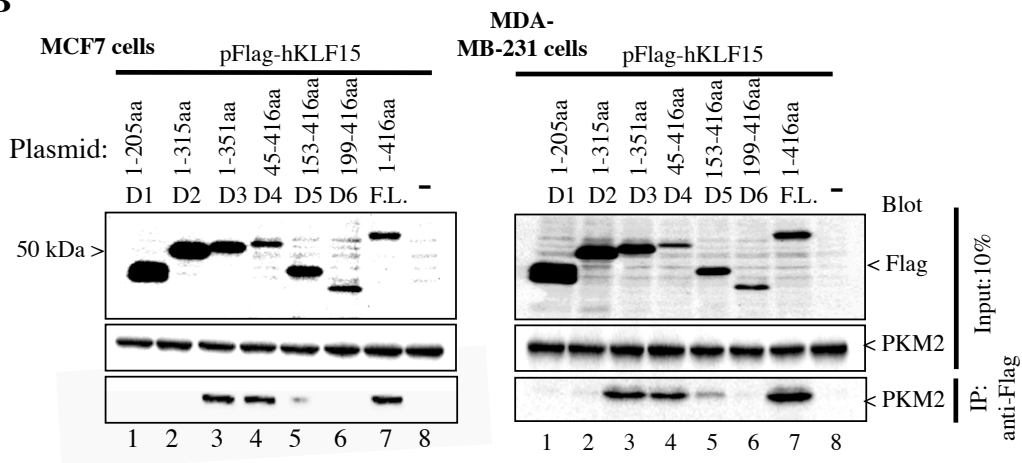
- (A) Schematic representation of primary structure of KLF15 and its deletion mutants.
- (B) Schematic representation of primary structure of PKM1 and PKM2, and their deletion mutants.
- (C) KLF15 interacts with N-terminal region (amino acids 1-377) of PKM2. COS7 cells were transiently transfected with the expression plasmids encoding HA-tagged KLF15 or its mutants along with the expression plasmids encoding Flag-tagged PKM1, PKM2, or its mutants as indicated. Whole cell extracts from the cells were immunoprecipitated with anti-Flag antibody. Ten percent inputs, eluates, and flow through fractions were separated with SDS-PAGE followed by western blotting analysis with anti-HA or anti-Flag antibodies. Representative images from three independent experiments are shown. IP: immunoprecipitation; F.T.: flow through.

Figure 6

A



B



C

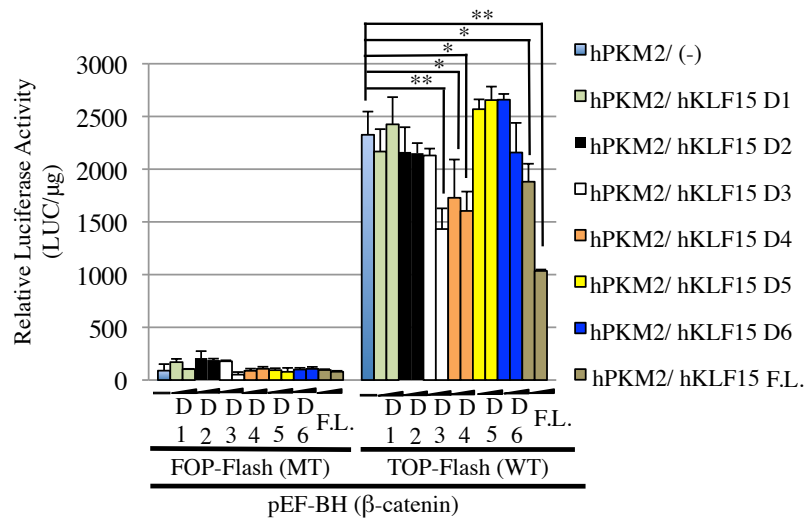
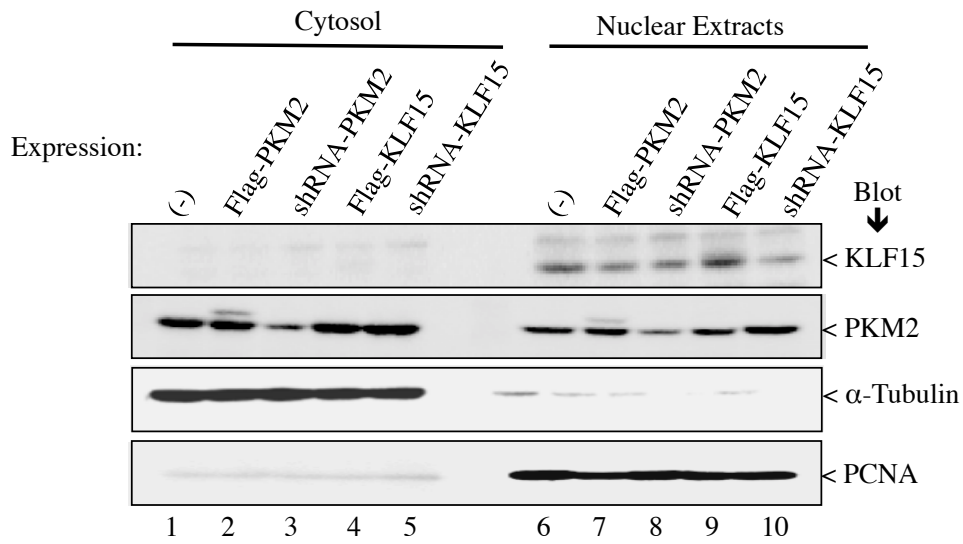


Figure 6. KLF15-PKM2 interaction downregulates β -catenin-dependent reporter gene expression in breast cancer cells

- (A) Schematic representation of Flag-tagged human KLF15 and its deletion mutants.
- (B) Flag-tagged human KLF15 (wild-type or its deletion mutants) was transiently overexpressed in MCF7 (left panels) and MDA-MB-231 (right panels) cells. Whole cell extracts from the cells were immunoprecipitated with anti-Flag affinity beads. Ten percent inputs and eluates were analyzed by western blotting. Representative images from three independent experiments are shown. IP: immunoprecipitation.
- (C) KLF15-PKM2 interaction contributes to suppression of β -catenin-dependent reporter gene expression. MCF7 cells were cotransfected with wild-type (TOP-Flash) or mutant-type (FOP-Flash) of β -catenin-dependent reporter gene, along with expression plasmids encoding β -catenin (pEF-BH), PKM2, or KLF15 (wild-type or its deletion mutants) as indicated. Luciferase activities are normalized to the amount of cellular proteins. Data represent the means \pm SEM of three independent experiments. *: $p < 0.05$; **: $p < 0.01$

Figure 7

A



B

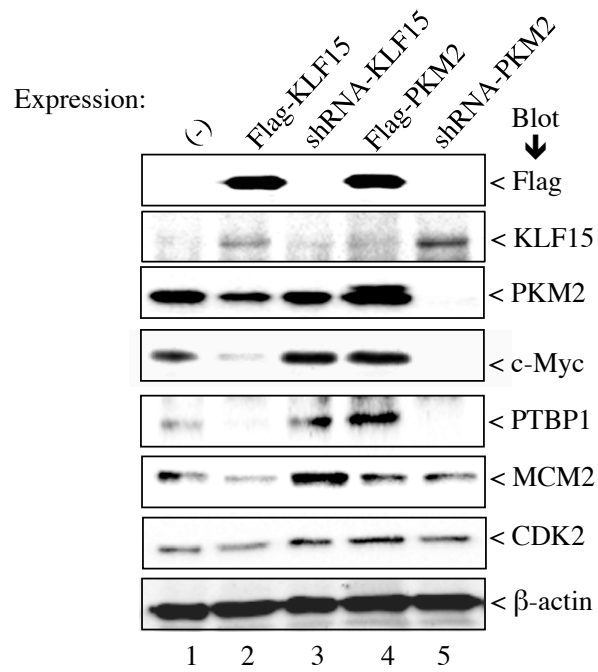
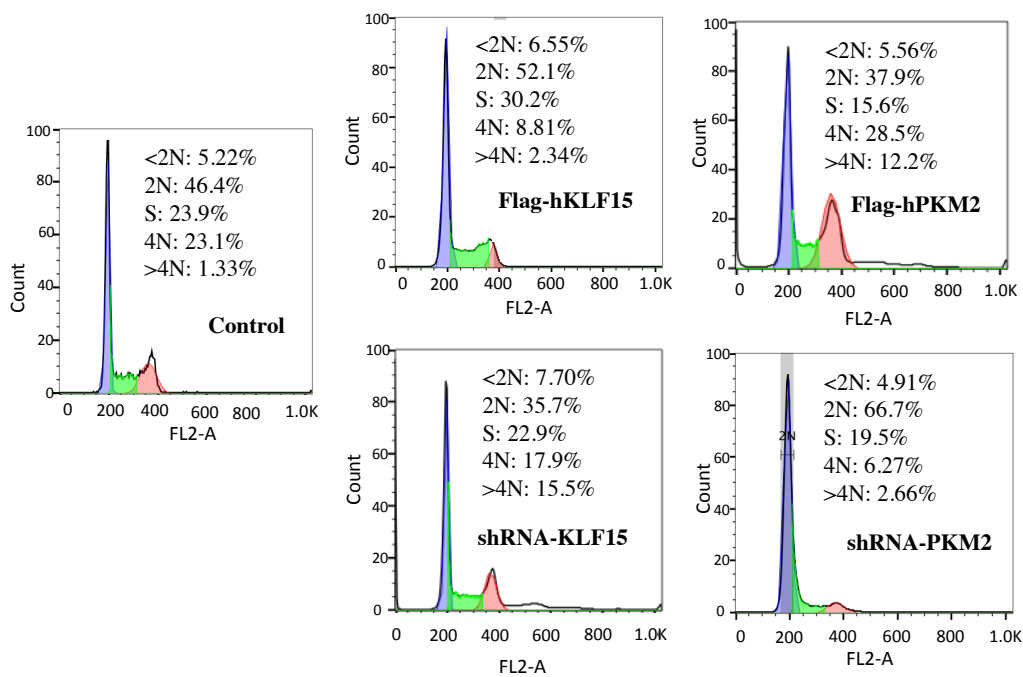


Figure 7. KLF15 and PKM2 regulate expression levels of several cellular proteins in human breast cancer cells

- (A) Characteristics of stably transfected human breast cancer cells. Nuclear extracts and cytosolic fractions from the indicated MCF7 cells were prepared, and subjected to western blotting analysis. Representative images from three independent experiments are shown.
- (B) Expression levels of various proteins in stably transfected MCF7 cells. Whole cell extracts from the indicated MCF7 cells were subjected to western blotting analysis with indicated antibodies. Representative images from three independent experiments are shown.

Figure 8

A



B

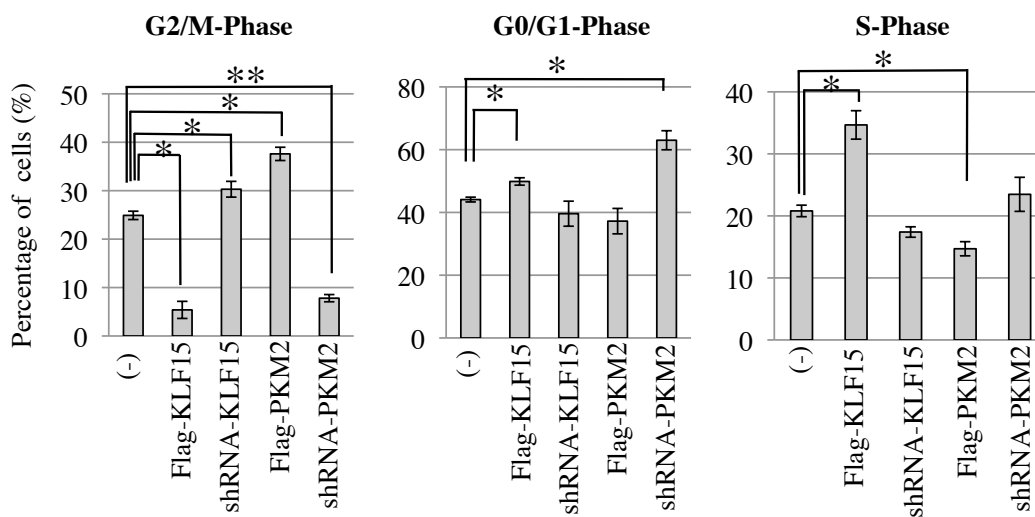
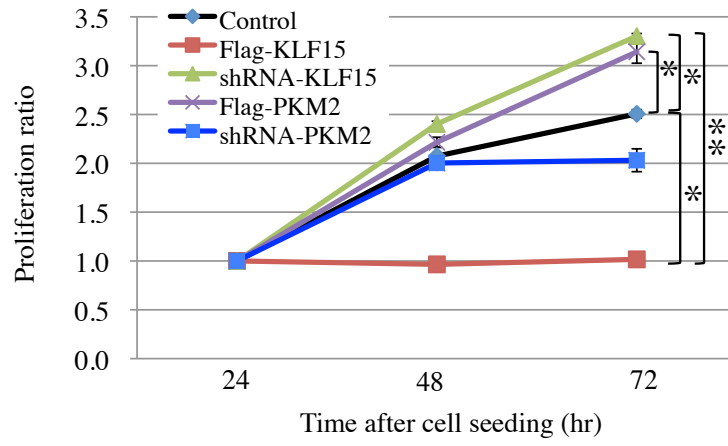


Figure 8. KLF15 and PKM2 regulate cell cycle distribution of human breast cancer cells

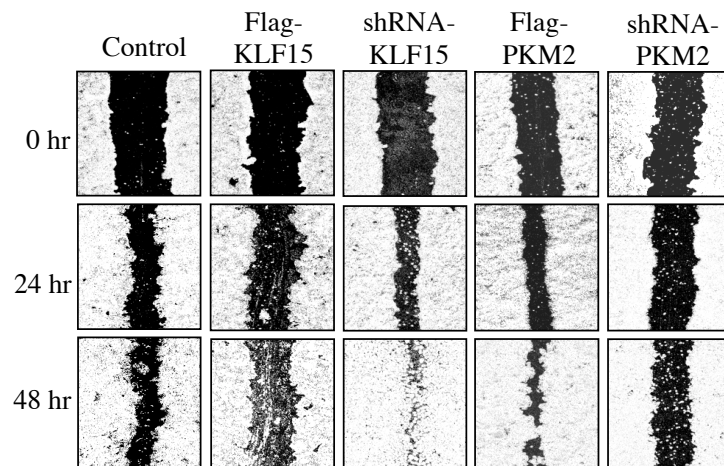
- (A) Cell cycle distribution of stably transfected MCF7 cells. To determine cell cycle distribution of stably transfected MCF7 cells, cells were harvested at the confluency of 80%, and subjected to flow cytometric analysis as described in Materials and Methods. Representative data from three independent experiments are shown. <2N: apoptotic cells; 2N: cell population in G0/G1 stage; S: cells undergoing DNA synthesis; 4N: cell population in mitotic stage; >4N: cells containing excess more than 4N DNA content.
- (B) MCF7 cells with KLF15-overexpression or PKM2-knockdown display G0/G1 phase-dominant distribution, accompanied by downregulated cell proportion in G2/M phase. The data obtained from flow cytometric analysis were calculated by Flow Jo software. Data shown represent the means \pm SEM from three independent experiments. *: $p < 0.05$; **: $p < 0.01$.

Figure 9

A



B



C

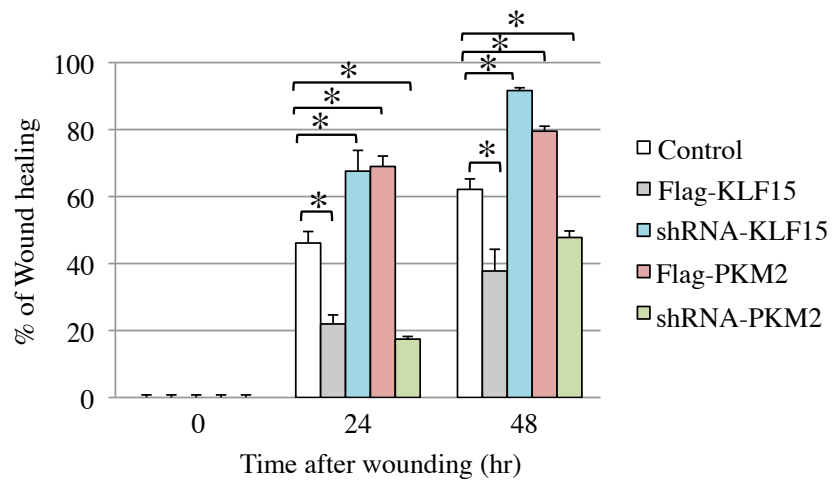


Figure 9. Either KLF15 overexpression or PKM2 knockdown suppresses breast cancer cell proliferation and migration

- (A) Effect of KLF15 and PKM2 on breast cancer cell proliferation. Stably transfected MCF7 cells as indicated were seeded in 96-well plate at 5000 cells/well. The number of the living cells was assessed with sensitive colorimetric assays at the indicated time points as described in Materials and Methods. Relative cell numbers compared with the values obtained at 24 hr-time point are presented (means \pm SD, n = 10). *: p < 0.05; **: p < 0.01.
- (B and C) Effect of KLF15 and PKM2 on breast cancer cell migration. Stably transfected MCF7 cells as indicated were incubated in 6-well tissue culture plates to reach 100% confluence. Wounds were created as described in Materials and Methods. Wound images were captured at 0, 24, and 48 hr after injury and wound areas were calculated by Image J software. Representative images were shown in (B). Wound healing rates are presented in (C). Data shown represent the means \pm SEM from three independent experiments with triplicate for each. *: p < 0.05

Figure 10

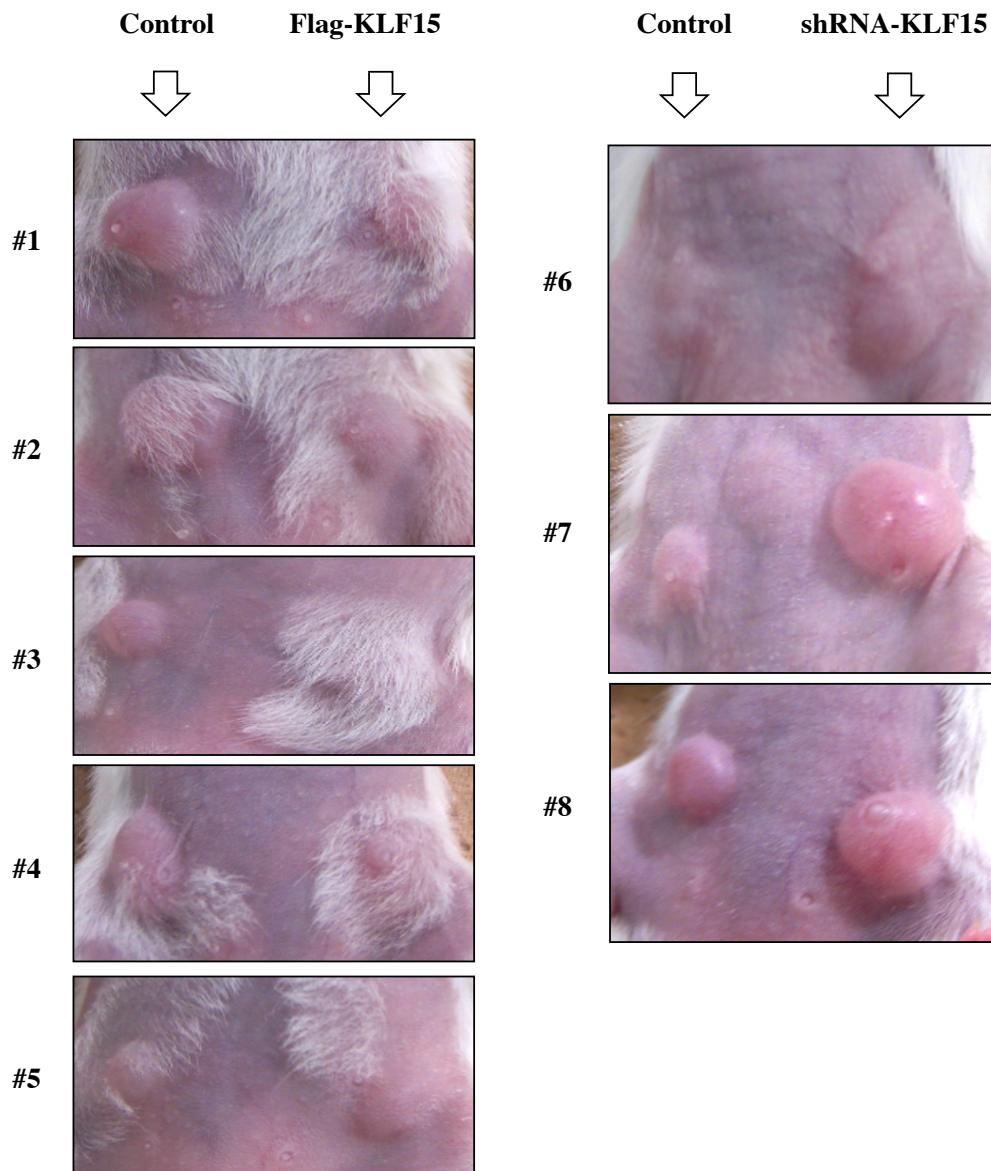
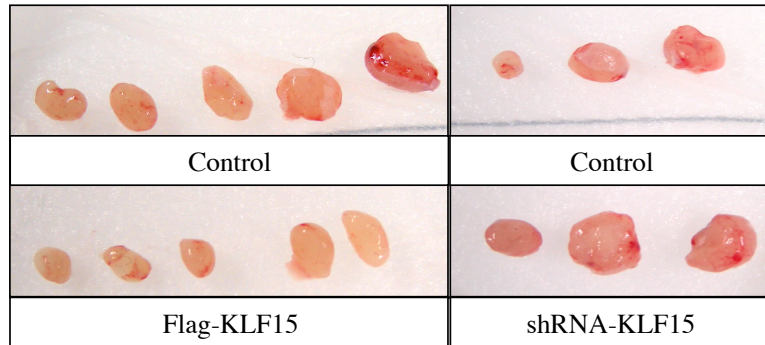


Figure 10. Xenograft transplantation of stably transfected MCF7 cells into NOD-SCID mice

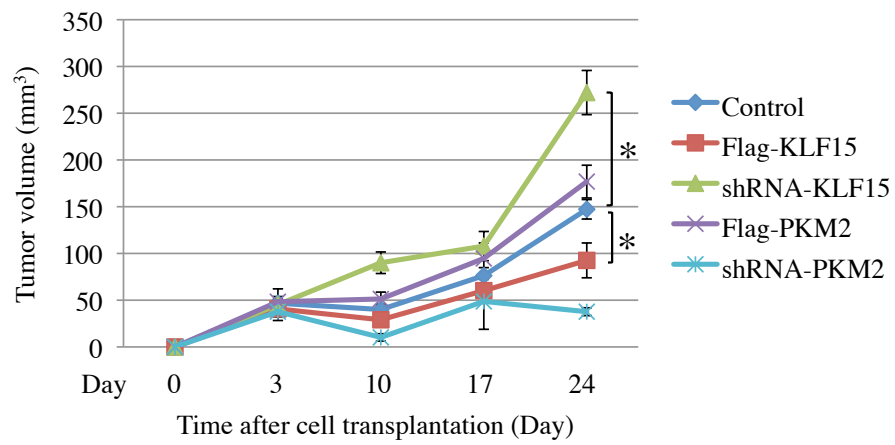
Negative control or stably transfected MCF7 cells as indicated were transplanted into the fourth inguinal mammary fat pad of NOD-SCID mice (1×10^6 cells each, with 50% v/v Matrigel). Tumor appearances at 24 days post-transplantation are shown.

Figure 11

A



B



C

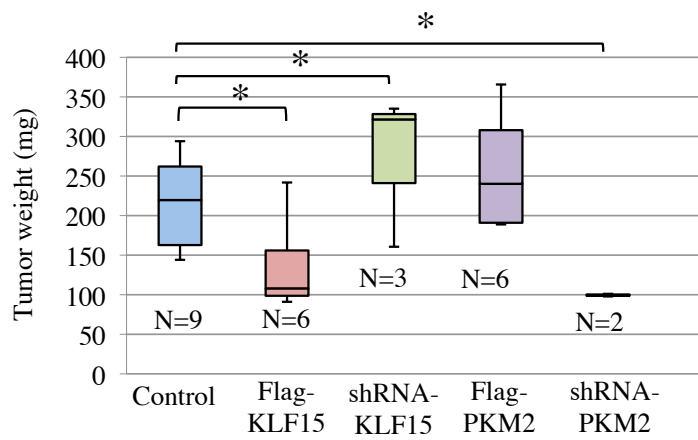


Figure 11. KLF15 suppresses and PKM2 promotes xenografted breast tumor growth in NOD-SCID mice

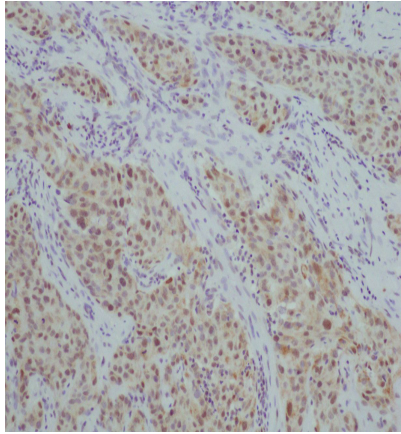
- (A) Negative control or stably transfected MCF7 cells as indicated were transplanted into NOD-SCID mice (1×10^6 cells each). At 31-day post-transplantation, the mice were sacrificed and xenografted tumors were harvested.
- (B) Negative control or stably transfected MCF7 cells as indicated were transplanted into NOD-SCID mice (1×10^6 cells each). Two dimensions of each tumor were monitored by caliper measurement at indicated time points. Tumor volume was calculated using the equation “ $V = (\pi/6) (\text{Length} \times \text{Width}^2)$ ”.
- (C) At 31-day post-transplantation, tumor xenografts were harvested. The tumor weights of each group were measured and shown by box plot.

Data shown represent the means \pm SEM (negative control: n=9; Flag-PKM2: n=6; shRNA-KLF15: n=3; Flag-KLF15: n=6; shRNA-PKM2: n=2). *: $p < 0.05$.

Figure 12

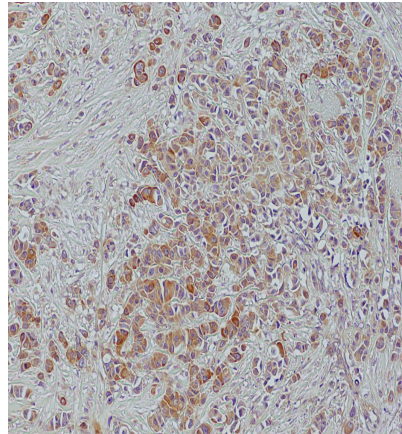
A

Anti-KLF15



100 μ m

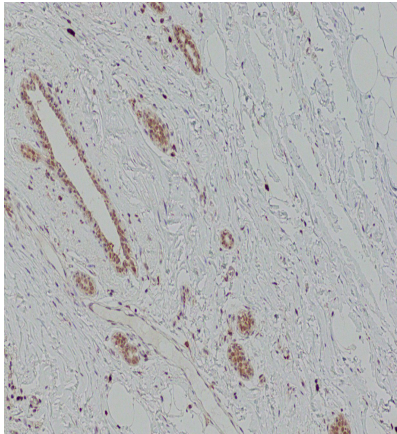
Anti-PKM2



100 μ m

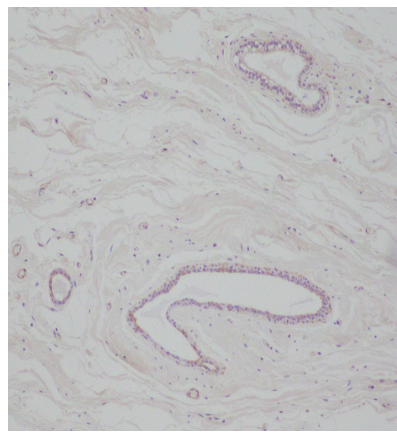
B

Anti-KLF15



100 μ m

Anti-PKM2



100 μ m

Figure 12. Immunohistochemical analysis of KLF15 and PKM2 in human breast carcinoma and non-neoplastic mammary gland tissues

To detect the expression of KLF15 and PKM2 in human breast carcinoma and non-neoplastic mammary gland tissues, 12 specimens of invasive ductal carcinoma of human breast were obtained from Japanese female patients who have not received chemotherapy. Immunohistochemical analysis was performed. Representative images of KLF15 and PKM2 expression in breast carcinoma tissues (**A**) and non-neoplastic mammary gland tissues (**B**) are shown.

Acknowledgements

First and foremost, I appreciate my mentor, professor Hirotohi Tanaka, for supporting my thesis work and encouraging me to think scientifically. I appreciate Dr. Noriaki Shimizu, Miss. Takako Maruyama, Dr. Noritada Yoshikawa and Dr. Hiroshi Kobayashi. I am grateful for the assistance and support of both past and present colleagues in the TANAKA laboratory (Department of Rheumatology and Allergy/Center for Antibody and Vaccine Therapy, IMSUT Hospital, the Institute of Medical Science, the University of Tokyo, Tokyo, Japan) for creating a unique atmosphere in which to perform research.

In addition, I am grateful for professor Takashi Suzuki and professor Shinichi Hayashi at Tohoku University Graduate School of Medicine (Sendai, Japan). I thank professor Shin'ichi Takeda and Dr. Naoki Ito at National Institute of Neuroscience, National Center of Neurology and Psychiatry (Kodaira, Tokyo, Japan). Furthermore, I would like to thank professor Masaaki Oyama of Medical Proteomics Laboratory at the Institute of Medical Science, the University of Tokyo (Tokyo, Japan).

I also want to thank my friend Li Wang at The University of Texas MD Anderson Cancer Center, Science Park Research Division (Smithville, Texas, USA). Finally, I also would like to thank my family, whose support has carried me through the past years.